Accepted Manuscript

Cosmic-ray-driven electron-induced reactions of halogenated molecules adsorbed on ice surfaces: Implications for atmospheric ozone depletion

Qing-Bin Lu

Please cite this article as: Q.-B. Lu, Cosmic-ray-driven electron-induced reactions of halogenated molecules adsorbed on ice surfaces: Implications for atmospheric ozone depletion, *Physics Reports* (2009), doi:10.1016/j.physrep.2009.12.002

PHYSICS REPORTS

SPIN OBSERVABLES AND SPIN STRUCTURE
FUNCTIONS: INEQUALITIES AND DYNAMICS

Available online at
ScienceDirect

Cosmic-Ray-Driven Electron-Induced Reactions of Halogenated Molecules Adsorbed on Ice Surfaces: Implications for Atmospheric Ozone Depletion

Qing-Bin Lu[*]

Department of Physics and Astronomy and Departments of Biology and Chemistry, University of Waterloo, Waterloo, ON, N2L 3G1, Canada

Abstract: The cosmic-ray driven electron-induced reaction of halogenated molecules adsorbed on ice surfaces has been proposed as a new mechanism for the formation of the polar ozone hole. Here, experimental findings of dissociative electron transfer reactions of halogenated molecules on ice surfaces in electron-stimulated desorption, electron trapping and femtosecond time-resolved laser spectroscopic measurements are reviewed. It is followed by a review of the evidence from recent satellite observations of this new mechanism for the Antarctic ozone hole, and all other possible physical mechanisms are discussed. Moreover, new observations of the 11-year cyclic variations of both polar ozone loss and stratospheric cooling and the seasonal variations of CFCs and CH$_4$ in the polar stratosphere are presented, and quantitative predictions of the Antarctic ozone hole in the future are given. Finally, new observation of the effects of CFCs and cosmic-ray driven ozone depletion on global climate change is also presented and discussed.

---

[*] E-mail: qblu@uwaterloo.ca

Contents

I. INTRODUCTION

Electron-transfer reactions play an important role in many processes in physical, chemical and biological systems [1-4] and planetary atmospheres [5-7]. Among electron-transfer reactions, dissociative electron transfer (DET) of molecules is one of the most important processes. Indeed, DET is a fundamental process involved in many areas of physics, chemistry, biology, environment and biomedicine, e.g., in atomic collisions with molecules [8], surface photochemistry [9, 10], atmospheric ozone depletion [11-17], electronic materials [18], femtochemistry and femtobiology [19-23], activation of anticancer drugs [21-23], and molecular pathways leading to DNA damage and cell death in the cellular (aqueous) environment [24].

In interactions of electrons with molecules, a well-known process is dissociative electron attachment (DEA). DET is similar to DEA, but there are some important differences. DEA occurs when a low-energy (0-20 eV) *free, unbound* electron resonantly attaches to a molecule to form a transient anion state, which then dissociates into a neutral and an anionic fragment: $e^- + AB \rightarrow AB^{*-} \rightarrow A + B^-$. The physical process of DEA has been comprehensively reviewed by Schultz [25], Sanche [26] and Chutjian et al. [6], respectively. In contrast, DET occurs by rapid electron transfer of *a weakly-bound electron* localized at an atom/molecule or in a polar medium to a foreign molecule, forming a transient anion that then dissociates. For those molecules having strong DEA resonances with free electrons at near zero eV in the gas phase, DET reactions can effectively occur when these molecules are adsorbed on metal surfaces [9, 10], polar ice surfaces [11-17] and in polar liquids [21-24, 27-29]. This is because the potential energy curve of AB^{*-} is lowered by the polarization potential E_p of $1-2$ eV to lie below that of the neutral AB in the Franck-Condon (electron-transition) region. This review will focus on experimental studies of DET reactions of halogenated molecules adsorbed on polar ice surfaces or in polar liquids. Taking CF_2Cl_2 adsorbed on the H_2O ice surface ($E_p \approx 1.3$ eV [30]) as an

example, the DEA and DET processes are illustrated in Fig. 1. In contrast to the DEA process, the lifetime of a weakly-bound trapped electron in polar media is orders of magnitudes longer than that of a free electron in the gas phase or a quasi-free electron in nonpolar media and the autodetachment of the AB^{*-} transient state once formed cannot occur in DET. These properties can greatly enhance the capture probability of the electron and the dissociation probability of the molecule in a DET reaction, as discussed recently [24, 29].

There is a long history of studying electron-induced reactions of halogenated molecules including chlorofluorocarbons (CFCs, the major ozone-depleting molecules), starting from gas-phase studies [31]. In particular, Illenberger et al. [32] first found in 1978-1979 that DEA of CFC molecules to low-energy free electrons near zero eV is an extremely efficient process, e.g.,

$$e^{-}(\sim 0eV) + CF_2Cl_2 \rightarrow CF_2Cl_2 *^{-} \rightarrow Cl^{-} + CF_2Cl. \tag{1}$$
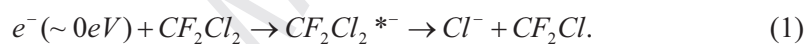
The above DEA reactions of CFCs are exothermic. The measured DEA cross section of gaseous CF_2Cl_2 (Eq. (1)) at near 0eV is $\sim 1 \times 10^{-16}$ cm^2, which is four orders of magnitude higher than the photodissociation cross section [32]. Immediately, Peyerimhoff and co-workers [33, 34] made the first theoretical studies of the DEAs of CFCs and pointed out that this process must be considered as a mechanism for the destruction of CFCs and the ozone layer in the stratosphere.

In the stratosphere below 60 km, the major source producing electrons is the atmospheric ionization by cosmic rays (CRs) [35, 36], which consist mainly of protons (90%) and alpha-particles (9%) originated from deep space. Entering the atmosphere, the ionization of molecules by CRs generates an enormous number of low energy secondary electrons. However, the detected density of *free* electrons is very low, as most of the free electrons produced by CRs are

rapidly captured by stratospheric molecules (mainly O_2) to produce negative ions (O_2^-). Since the electron transfer from O_2^- to CFCs is ineffective, the DEA/DET process was thought to be an insignificant sink for CFCs in the general atmosphere [35, 36]. Although it was generally agreed that this understanding of negative-ion chemistry in the stratosphere was rather speculative [35, 36], the DET process has been excluded in current atmospheric chemistry models [37]. As will be reviewed below, however, a neglect of electron-induced reactions of halogenated molecules as an efficient process for the destruction of the ozone layer may be premature.

Correct understanding of how ozone holes are formed and how that relates to climate change is without doubt of great significance. The data from satellite, ground-based and balloon measurements have confirmed that anthropogenic emissions of CFCs and hydrochlorofluorocarbons (HCFCs) are related to stratospheric ozone loss, and the Montreal Protocol has successfully phased out the production and consumption of these chemicals. However, it is still required to obtain both correct and complete ozone depletion theory and precise atmospheric measurements in order to put the Protocol on a firmer scientific ground [38, 39]. This review is organized as the following structure. The photochemical model for the ozone hole, the cosmic-ray-driven electron-induced reaction mechanism (denoted as the "CRE" model hereafter) and the more recent justification of the CRE mechanism are briefly reviewed in Section II. It is followed by a review of laboratory findings of electron-induced reactions of CFCs, HCFCs and other halogenated molecules adsorbed on polar ice surfaces or in polar liquids in Section III. Section IV gives a review of the evidence from satellite data of the CRE model for Antarctic ozone depletion, and all possible physical mechanisms rather than the CRE model are discussed. New observations of the 11-year cyclic variations of both polar O_3 loss and stratospheric cooling, as well as the seasonal variations of CFCs and so-called trace gases (N_2O

and CH$_4$) in the polar stratosphere, are presented in Section V. Then, quantitative analyses of the available O$_3$ data from satellite and ground-based measurements in the Antarctic stratosphere in 1956-2008 are presented in Section VI. It follows by Section VII to give quantitative predictions of the Antarctic O$_3$ hole in 2009~2010 and its future trend towards the 21st century. Finally, new observation of the co-effects of CFCs and CR-driven ozone loss on global climate change is presented in Section VIII, ending with the conclusions in IX.

II. COSMIC-RAY-DRIVEN-ELECTRON-REACTION MODEL VS PHOTOCHEMICAL MODEL FOR OZONE DEPLETION

A. Photochemical Model for Ozone Depletion

In 1974, Molina and Rowland [40] first proposed that chlorine atoms are produced by sunlight *photolysis* of CFCs in the tropical upper stratosphere at ~40 km:

$$CF_2Cl_2 + h\nu \rightarrow Cl + CF_2Cl. \tag{2}$$

The resultant Cl atom then destroys ozone via the (Cl, ClO) reaction chain, similar to the destruction of O$_3$ via the (NO, NO$_2$) reaction chain first proposed by Crutzen in 1971 [41]. However, the ozone hole has been observed in the lower stratosphere at ~18 km over the Poles in each spring since the first discovery of the Antarctic ozone hole in 1985 [42]. A mixed mechanism was subsequently proposed, which is composed of three major processes (see, e.g., refs. 43 and 44): (1) the *photolysis* of CFCs produces Cl and ClO that react with other atmospheric molecules (CH$_4$ and NO$_2$) to generate inorganic chlorine species, HCl and ClONO$_2$,

in the tropical upper stratosphere at the altitudes of ~40 km; (2) HCl and ClONO$_2$ were then transported to the lower polar stratosphere via *air circulation*; and (3) *heterogeneous chemical reactions* of these inorganic compounds on ice surfaces occur in the lower polar stratosphere (15-20 km) during winter:

$$HCl(s) + ClONO_2(g) \rightarrow Cl_2(g) + HNO_3(s) \qquad (3)$$

(s, solid; g, gas). Step (3) converts the inactive chlorine compounds into photo-reactive species (Cl$_2$). In the winter lower polar stratosphere, a strong polar vortex isolates a continent-size body of air, in which polar stratospheric clouds (PSCs) of several km in thickness form due to very low temperatures [44, 45]. These PSCs consist of water ice or nitric acid/ice particles with a major composition of H$_2$O. In the photochemical model, Eq. (3) is thought to be the major mechanism for the activation of inert halogenated compounds into photoactive halogens in PSCs in the dark polar stratosphere during winter, a key step for the subsequent formation of the springtime ozone hole [44, 45]. When sunlight returns in spring, Cl$_2$ releases chlorine atoms to destroy O$_3$ in the polar stratosphere.

B. **Cosmic-Ray-Driven-Electron-Reaction Model for Ozone Depletion (CRE)**

The study of the implications of electron-induced reactions of halogenated molecules for stratospheric ozone depletion has revived since the reporting of large enhancements in electron-induced dissociations of CFCs by the presence of polar molecular ices in 1999 [11, 12]. The original project aimed to study elastic and inelastic processes of low-energy ions transmitting

through ultrathin surface layers (Ar, Kr, Xe, H_2O and NH_3) [46]. Unexpectedly, Lu and Madey observed that the anion (Cl^- and F^-) yields in electron-stimulated desorption (ESD) of CFCs are enhanced by up to four orders of magnitude when CFCs are coadsorbed with polar molecular ice (H_2O, NH_3) on a Ru(0001) surface [11, 12]. To find a mechanism to explain the observed results, Lu and Madey noticed a basic fact that an excess electron can become self-trapped (solvated) in a polar medium. The solvated electron was first observed in liquid NH_3 by Weyl in 1863 [47] and in liquid H_2O by Boag and Hart about 100 years later [48]. The advent of femtosecond ($1fs=10^{-15}$ s) time-resolved laser spectroscopy in 1987 provided a new-level understanding of the dynamics of electron solvation in water, as first studied by Migus et al. [49]. By the end of 1990s, it became clear that prior to the formation of the equilibrium-state solvated electron (e_{sol}^-), the excess electron in bulk water is located at precursor states with finite lifetimes less than 1 picosecond ($1ps=10^{-12}$ s), the so-called prehydrated electron (e_{pre}^-) [49-54]. And negatively charged water clusters $[H_2O]_n^-$ (n=2-69) were also first observed by Haberland and Bowen's groups in 1980s-1990s [55, 56]. On the basis of these previous findings, Lu and Madey [11, 12] proposed a *dissociative electron transfer* (DET) mechanism to explain their observations of large anion-yield enhancements: secondary electrons from the metal are first trapped in polar media and then transferred to CFCs that dissociate to form anion fragments.

Lu and Madey [12] also noticed the fact that polar stratosphere clouds consisting of ice particles exist in the winter polar stratosphere, making it different from the general stratosphere. Consequently, the CR-induced physics and chemistry of molecules in the winter polar stratosphere can be drastically different from that in the general stratosphere without the presence of polar stratosphere clouds. Inspired by the finding of Finlayson-Pitts and co-workers

[57] that anions can enhance the generation of reactive chlorine from sea salts in the atmosphere in 1998, Lu and Madey [12] explored the implications of their finding of anionic (Cl^-) enhancements for ozone depletion in the polar stratosphere. They proposed that the resultant Cl^- ions can be converted to Cl atoms to destroy O_3 molecules, or the reactions of Cl^- with stratospheric species can result in the formation of photoactive Cl_2, $ClNO_2$ or $OClO$ in the winter polar stratosphere [12]. Upon photolysis in spring, these molecules release Cl atoms to destroy O_3 in the polar stratosphere. The last step is similar to the photochemical model described previously.

In 2001, Lu and Sanche confirmed the DET reactions of halogenated molecules adsorbed on ice film surfaces by studying the trapping of near zero eV electrons at presolvated surface states and the transfer to CFCs or HCl adsorbed on ice surfaces [13]. They also studied the relevance of the cosmic-ray driven DET reactions to CFC dissociation and ozone depletion in the stratosphere [14]. Further, Lu [15] has recently shown strong evidence of the CRE mechanism for polar ozone depletion from the satellite data over two 11-year CR cycles (1979-2007). The CRE mechanism, as schematically shown in Fig. 2, has therefore been developed [12, 14, 15].

The CRE mechanism drastically differs from the photochemical model for stratospheric ozone depletion. The latter assumes that the sunlight photolysis of CFCs in the upper tropical stratosphere, air transport and the subsequent heterogeneous chemical reactions of transported inorganic halogens on ice surfaces in PSCs are the three major processes for the activation of halogenated compounds into photoactive halogens. In contrast, the CRE model believes that the *in-situ* CR-driven electron-induced reaction of halogenated molecules including organic and inorganic molecules (CFCs, HCl, $ClONO_2$, etc) adsorbed or trapped at PSC ice in the winter

polar stratosphere is the key step to form the photoactive halogen species that then lead to the springtime ozone hole.

C. More Justification of the Cosmic-Ray-Driven-Electron-Reaction Model

In 2000s, Researches on electron solvation dynamics and associated dissociative electron transfer reactions of halogenated molecules have continued in water solution [21, 27-29, 58-62], ice surface [63], ultrathin ice films [16, 17, 64-67] and H_2O anionic clusters [68-73]. Prior to 2008, many experimental and theoretical studies gave very diverse lifetimes and physical natures of e_{pre}^- states in liquid water [49-54, 58-62]. But Wang et al [28] have recently resolved that e_{pre}^- states are electronically excited states and have lifetimes of ~200 and 500 fs after the identification and removal of a coherent spike effect. The e_{pre}^- lifetime of ~500 fs is consistent with the theoretical prediction by Rossky and Schnitker [50] and recovers the earlier result observed by Long et al. [51]. The coherent spike effect has recently been found in other (many) pump-probe spectroscopic measurements [74]. Earlier femtosecond time-resolved spectroscopic studies by Wolf's group [64] and Petek's group [65] on thin amorphous ice films (a few monolayers) on a metal or insulator substrate showed lifetimes of less than 1 ps for the presolvated electrons. By first-principles molecular dynamics simulations of the ice surface at the temperatures close to those found in PSCs (150-200 K), Baletto et al. [63] found very stable surface-bound states for trapping electron at the ice surface due to the structural rearrangement induced by an excess electron. They proposed that the surface molecular rearrangement leads to an increase of the number of dangling OH bonds pointing towards the vacuum and to the formation of an electrostatic barrier preventing the decay of the electron into the bulk solvated state [63]. Most recently, interesting results were reported by Wolf, Bovensiepen and co-

workers [17, 67], who observed long-lived trapped electrons with a lifetime up to minutes at the crystalline ice surface. They also performed first principle calculations, which lead to a conclusion that the observed long-lived trapped electrons is due to electron trapping at pre-existing structural defects on the surface of the crystalline ice [67]. The above-mentioned results have provided a strong foundation for the CR-driven DET reaction mechanism of halogenated molecules adsorbed/trapped at ice surfaces in PSCs. As mentioned above, DEAs of many Cl-, Br- and I-containing molecules (particularly CFCs) are exothermic, and therefore DEAs of these molecules can occur at zero eV electrons in the gas phase [31, 32]. The exothermic energies of the DEA reactions on H_2O ice or in liquid water will be enhanced by 1−2 eV due to the effect of the polarization potential [30], as shown in Fig. 1. This leads to strong resonances of anion states of Cl-, Br- and I-containing molecules with e_{pre}^- that is weakly-bound at −1.5 to −1.0 eV [13, 16, 17, 21, 27-29]. Thus, quite effective resonant DET can occur for organic and inorganic (ozone-depleting) halogenated molecules (CFCs, HCl, $ClONO_2$, etc) on H_2O ice, as demonstrated in the experiments to be reviewed in next Sections.

III. LABORATORY FINDINGS OF DISSOCIATIVE ELECTRON TRANSFER REACTIONS OF HALOGENATED MOLECULES ON ICE

A. Electron-stimulated desorption (ESD) measurements

To generate low-energy anions and study the physical processes in their transport through surface overlayers [46], Lu and Madey [75] first studied anion formation in electron-stimulated desorption (ESD) of CF_2Cl_2 adsorbed on a Ru(0001) surface with an incident electron beam at hundreds of eV. They found that the anions (Cl^- and F^-) were mainly generated by DEAs to CF_2Cl_2 of low-energy secondary free electrons emitted from the metal substrate. Unexpectedly they observed a striking effect that the yields of anions are enhanced by orders of magnitude

when CF_2Cl_2 is coadsorbed with ~ 1 monolayer of polar molecular ice (H_2O, NH_3) on the metal exposed to an electron beam of 250 eV [11, 12]. The experiments were conducted in an ultrahigh vacuum (UHV) chamber with a base pressure ~4×10^{-11} torr. A highly sensitive electron stimulated desorption ion angular distribution (ESDIAD) detector with time-of-flight (TOF) capability permits direct measurement of the total yield and the angular distribution of a specific ion species [76]. The ESDIAD/TOF detector, as shown in Fig. 3, is composed of a set of four high transparency planar grids of which all except the second are grounded, a array of five microchannel plates, and a position sensitive resistive anode encoder (RAE). The RAE is connected to a position analyzing computer to provide direct digital acquisition of two-dimensional data. By pulsing the primary electron beam and gating the retarding potential at grid G, one can obtain an extremely high detection efficiency for desorbing ions. In the experiments of Lu and Madey, the electron beam size was ~1mm, the used electron current was adjustable between 0.05 nA and 20 nA, depending on CF_2Cl_2 precoverage, and the collection time for each data point was *5 seconds only*, to avoid detector saturation and to minimize beam damage [11]. For the observations of giant Cl^- enhancements up to 10^4 in the ESDIAD measurements, *low electron currents (≤1 nA)* were used. The coverages of CF_2Cl_2 and polar molecules were carefully determined from temperature programmed desorption (TPD) spectra, where one monolayer (ML) of H_2O refers to a bilayer with a density of ~1.0×10^{15} molecules.cm^{-2} and one ML of CF_2Cl_2 is defined as the coverage corresponding to the saturation of the monolayer peak in TPD spectra, i.e., the onset of the multilayer peak [75].

The variations of the Cl^- yield versus H_2O and NH_3 film thickness for various CF_2Cl_2 pre-coverages are reproduced as Fig. 4. In the case of H_2O coadsorption, it is seen that for the lowest CF_2Cl_2 coverages, the Cl^- yield increases greatly with the initial coadsorption, exhibits a

maximum enhancement by nearly two orders of magnitude at about one ML of H_2O, and finally decreases to zero intensity at ~4.0 ML H_2O overlayer. With higher H_2O thickness, the Cl^- yield decreases, which is expected due to elastic and inelastic scattering as the desorbed ions pass through the H_2O film. Similar results were observed for the coadsorption of NH_3, but the enhancement is about two orders of magnitude larger than for H_2O coadsorption: the maximum Cl^- enhancement for 0.3 ML CF_2Cl_2 is a factor of ~$3x10^4$. Also, F^- enhancements were observed for either H_2O or NH_3 coadsorption, but the magnitude of enhancement for F^- is much smaller than for Cl^- with an identical CF_2Cl_2 coverage [11, 12].

Similar anion enhancements were observed for ESD of 0.3 ML CF_2Cl_2 adsorbed on top of H_2O-precovered Ru surfaces with various H_2O thickness [12]; the variation of the Cl^- desorption yield is reproduced as Fig. 5. At the H_2O coverage of ~1 ML, the Cl^- yield exhibits a maximum of two orders of magnitude higher than that without the presence of H_2O. With larger H_2O spacer thickness, the Cl^- yield decreases. This is due to the finite tunneling depth (2~4 ML) of low-energy secondary electrons from the substrate through the ice film [77, 78]. The higher desorbed Cl^- yield for CF_2Cl_2 adsorbed on top of a water-ice surface (Fig. 5) than for its coadsorption with water on a metal substrate (Fig. 4) is due to a lower ion scattering loss probability and a lower image-potential attraction (a higher desorption probability) on the water-ice surface than on the metal substrate [12].

One has to consider the possible effects of the metal substrate on the observed anion enhancements in the above ESD experiments. However, the F^- yield enhancements are much smaller than those of the Cl^- yield, and much smaller F^- and Cl^- enhancements (less than one order of magnitude) were observed when CF_2Cl_2 was coadsorbed with non-polar molecules such as rare-gas molecules (Xe, Kr and Ar) on Ru [11, 79, 80]. These facts led to the conclusion that

the metal substrate could only play a minor role (such as through work-function-variation and image-potential effects) in enhancing the anion yields by the presence of polar H_2O/NH_3 ice [80].

Interestingly, Cowin and co-workers [81] observed electron-induced dissociation of CH_3Cl on Ni(111) under UV irradiation, though it was not clear whether the fragment of CH_3 resulted from the DEA of a low-energy photoexcited free electron or from the DET of a weakly-bound subvacuum photoexcited electron from the metal. More interestingly, they also observed a similar enhancement by ~50 times of the yield of the *neutral* CH_3 fragment in photoreduction of CH_3Cl adsorbed on Ni(111) surface with the presence of ~1 ML H_2O spacer layer [77]. The CH_3-yield enhancement then quickly decreased with increasing H_2O thickness and was about one order of magnitude lower at 5 ML H_2O due to the limited tunneling depth (2~4 ML) of low-energy electrons in ice. This is quite similar to the observed ESD Cl^--yield enhancements shown in Fig. 5, though the CH_3Cl coverage was not given in ref. 77. Gilton et al. [77] attributed the CH_3-yield enhancement to a strong inelastic scattering interaction between the photoexcited electrons and the H_2O, compared with the monotonic and slow decrease of the CH_3 signal with increasing Xe spacer thickness. This interpretation without involving trapped electrons and DET, however, cannot explain the observed much larger anion enhancements in electron-induced dissociation of CF_2Cl_2 by the presence of NH_3 than by H_2O, since inelastic electron scattering by NH_3 (with a dipole moment of 1.47 D) is weaker than by H_2O (1.84 D) [11].

In fact, polar NH_3 has long been employed as a reagent gas to enhance the detection sensitivity of organic and inorganic halogenated molecules in ammonia-enhanced anion mass spectrometry though the role of NH_3 was unknown there [82, 83]. And the solvation of electrons generated by adding electron donors (alkali metals) into polar media such as liquid ammonia had

been adopted as an effective method for dehalogenation of environmentally hazardous halogenated materials including CFCs. In the latter, halogen atoms were reduced to halogen ions and dechlorination of CFCs was also observed to be much more efficient than defluorination [84, 85]. Realizing these observations, Lu and Madey [11, 12, 79, 80] proposed a *dissociative electron transfer* mechanism to explain the observed anion enhancements in ESD of CFCs adsorbed on polar ice surfaces. They proposed that secondary electrons with energies of nearly 0 eV, produced by bombardment of the metal substrate with high-energy (250 eV) electrons, are injected and trapped in the polar molecular (H_2O/NH_3) layer; the giant anionic enhancements are due to transfer of trapped electrons (e_t^-) in polar ice to CFCs that then dissociate into Cl^- and a neutral fragment. The DET process, e.g. for CF_2Cl_2, can be expressed as [11, 12, 79, 80]:

$$e^- + mNH_3 / nH_2O \rightarrow e_t^-(NH_3)_m / e_t^-(H_2O)_m, \tag{4}$$

$$e_t^- + CF_2Cl_2 \rightarrow CF_2Cl_2 *^- \rightarrow Cl^- + CF_2Cl. \tag{5}$$
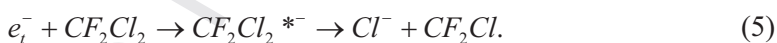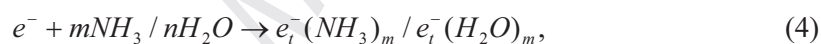
In contrast to e_t^- in polar media, low-energy secondary electrons in nonpolar media (e.g., rare-gas films) remain quasi-free and thus have extremely short residence times (lifetimes) in femtoseconds, decaying quickly into the metallic substrate without transfer to CFCs. Therefore the anionic enhancements via the DET mechanism in nonpolar media is very limited, in spite of the fact that coadsorption of rare-gas atoms leads to a larger yield of secondary electrons from the metal substrate [80]. Moreover, according to the DET mechanism, the anion enhancement factor Φ can be expressed as: $\Phi=(D_1+D_2)/D_1=1+ D_2/D_1$, where D_1 is the amount of CFC molecules dissociated by DEA of low-energy free electrons from the metal and D_2 the amount of CFC molecules dissociated by DET of trapped electrons in ice. D_1 is usually proportional to the

CFC coverage unless all secondary electrons are depleted (not the case under normal experimental conditions). However, it should be noted that only a small percent of low-energy free electrons become trapped electrons in the ice layer of ~1ML and they have a much longer lifetime to react with CFC molecules. Thus, there is an upper limit for the D_2 value: the maximum value, $(D_2)_{max}$, is equal to the total number of trapped electrons, which depends on specific experimental conditions. This will lead to a result that at very low CFC coverages, the D_2 is proportional to the CFC coverage; at high CFC coverages, $D_2=(D_2)_{max}$. Consequently, the anion enhancement factor Φ should decrease with increasing CFC coverages at the intermediate coverages and $\Phi\approx1$ (no enhancement) at high CFC coverages. This is in good agreement with the observed data (Fig. 4) [11, 12, 79, 80].

Most of the Cl^- ions from the DET reaction in Eqs. (4) and (5) are trapped at the surface by the image potential, as the desorption probability of Cl^- ions resulting from near 0 eV electrons is extremely low (10^{-7}–10^{-6}) [9, 12]. The measurement to obtain a sufficient Cl^- signal has therefore been a quite challenging task. Only a few groups in the worldwide have been able to detect the extremely low Cl^- yields produced by DEAs/DETs of molecules with ~0 eV electrons on metal surfaces. Polanyi and co-workers [9, 10] were the first to directly observe desorption of Cl^- ions from photoinduced DETs of weakly-bound hot electrons (<0 eV) at a metallic substrate to CCl_4 and chloromethanes adsorbed on the surface. Fortunately, another system equipped with an extremely sensitive ESDIAD/TOF detector (Fig. 3) [75, 76] was available in the system operated by Lu in Dr. Madey's laboratory at Rutgers in late 1990s. For detection of negative ions with an extremely low yield, a pulsed gating technique must be applied to close the detector when a large number of secondary electrons generated by primary electrons/photons arrive at the detector, i.e., to open the detector just before the arrival of anions to be detected. This can avoid

over-warming (pre-saturation) at the detector when a high voltage is applied to achieve the highest detection efficiency. The relatively unique facility at Rutgers allowed one to observe true DET reactions of intact CFCs with low electron doses, avoiding the effects of their reaction products and sample damage. Note that the DET cross sections of CF_2Cl_2 adsorbed on H_2O ice, after removing the possible effects of the metal substrate, was measured to be $\sim 1 \times 10^{-14}$ cm^2, which is *six orders of magnitude* higher than the photodissociation cross section (10^{-20} cm^2) of CF_2Cl_2 [12]. Thus, a very low electron dose must be used to make the measurements.

After the finding of Lu and Madey [11, 12], Langer et al. [86] reported no anion enhancements for electron-induced reactions of CF_2Cl_2 with NH_3 but their experimental conditions were very different from those of Lu and Madey. In those gas-phase or cluster experiments, two problems should be noted. First, the detection system of Langer et al was a commercial quadrupole mass spectrometer (QMS) and did not have the capability to detect desorbing Cl$^-$ ions resulting from DEA/DET resonances at near 0 eV on a metal surface, even for thick multilayers of adsorbed CF_2Cl_2 with a high electron current of 40-50 nA. Langer et al thus concluded that "desorption at very low electron energies is not operative" [86]. Second, detailed TPD spectra of CF_2Cl_2 adsorbed the surface were not recorded in those experiments, which are often required to determine adsorbate coverages reliably.

The negative results of Langer et al [86] stimulated Solovev et al. [87] to revisit the ESD experiments using both ESDIAD and higher-sensitivity QMS systems. The latter was modified to have the TOF capability by using a pulsed electron beam and a pulsed detector gate. The results of Solovev et al. [87] is reproduced as Fig. 6, which have substantially confirmed the giant Cl$^-$ enhancements by $>10^3$ times for submonolayers of CF_2Cl_2 co-adsorbed with NH_3 on Ru(0001), originally observed by Lu and Madey [11, 12]. Solovev et al. also observed some

differences: the Cl^- enhancements observed by the QMS detector, are significantly smaller those with the ESDIAD detector, e.g., the Cl^- enhancement factor at 1 ML CF_2Cl_2 by 1.5 ML NH_3 coadsorption decreased from 150~200 to less than 50. These differences were attributed to technical origins such as mass resolution, background subtractions and different collection angles for QMS and ESDIAD detectors [87]. Unfortunately, a key experimental difference was not mentioned. The ESDIAD detector at Rutgers [75, 76, Fig. 3] has an extremely high sensitivity, orders of magnitude higher than the QMS detector with a single channel electron multiplier at Rutgers and probably in most commercial QMS systems. Thus, the required electron dose with the ESDIAD detector is much lower than that required by a QMS. High electron doses can cause significant damage to the sample, in particular when DET cross sections of CF_2Cl_2 are greatly enhanced up to $10^{-14} - 10^{-13}$ cm^2 by H_2O and NH_3 [11, 12]. For those experiments, low electron doses $\leq 1 \times 10^{12}$ cm^2 are required to achieve reliable measurements. Lu and Madey were aware of this critical condition, and hence low electron currents (≤ 1 nA) and a short data correction time of only 5 s were used for detection of the maximum Cl^- enhancements up to 10^4 in their ESDIAD experiments [11, 12, 79, 80]. Notably, Solovev et al. [87] used the same facility with similar electron currents but a data collection time of 60 s, one order higher than that used by Lu and Madey. This can reasonably explain the slight differences in ESDIAD results: at high CF_2Cl_2 coverage (1 ML) the maximum Cl^- enhancement by ~1 ML NH_3 measured by Solovev et al. (Fig. 5b) is no less than that observed by Lu and Madey (Fig. 4b), but at the lowest CF_2Cl_2 coverage (0.3 ML) a smaller maximum Cl^- enhancement was measured by Solovev et al. The most likely origin is that for 0.3 ML CF_2Cl_2, an electron current much larger than that for 1ML CF_2Cl_2 was required and a significant decomposition of the CF_2Cl_2 coadsorbed with ~1 ML NH_3 could not avoided even within a

single measurement (60 s) if the electron beam current was not reduced. Overall, it is not surprising to observe smaller anion enhancements with a QMS than with an ESDIAD detector, since the former required a much larger electron dose and tended to cause damage to the sample.

Remarkably, the advantage of these ESD experiments is the capability of directly measuring the dissociation products (anions) from the DET reactions. On the other hand, it requires an anion detector of an extremely high sensitivity, and cautions must be taken to remove the effects of the metal substrate and the potential artificial effects mentioned above in order for reliable determination of the absolute DET cross sections [80].

B. Electron trapping measurements

In 2000-2001, Lu and Sanche [13, 88-90] directly used a low-energy (0-10 eV) electron beam reaching zero eV to examine the DET mechanism for large enhancements in dissociation of halogenated molecules (CFCs, HCFCs and HCl, etc) adsorbed on ice films. As shown in Fig. 7, a Kr spacer film of 10 ML was used to isolate any possible effects of the Pt substrate and to facilitate the growth of a uniform H_2O/NH_3 film. In the experiments, electron trapping in a dielectric film was measured by the low energy electron transmission (LEET) method [91]. A magnetically collimated electron beam (0-10 eV) having an energy resolution of 40 meV is produced by a trochoidal monochromator. A LEET spectrum records the electron current transmitted through a dielectric film as a function of incident electron energy E, which has a sharp onset at the vacuum level defined as zero eV. If electrons are trapped in the film with a lifetime longer than the detection limit of ms, the onset curve shifts to a higher energy by ΔV. An electron trapping coefficient $A_s(E)$ is defined as $d(\Delta V)/dt$ at t=0. For charging by a submonolayer

of CF_2Cl_2 on the H_2O or NH_3 film surface, the electron-trapping cross section $\sigma(E)$ is obtained by [13, 88-90]

$$A_s(E) = \frac{\sigma(E)\rho_o J_o}{\varepsilon_o}(\frac{L_1}{\varepsilon_1} + \frac{L_2}{\varepsilon_2}). \tag{6}$$

Here, ρ_0 is the surface density of electron-trapping molecules, J_0 the incident electron density and ε_0 the vacuum permittivity. ε_1 (1.91) and ε_2 (3.3 and 3.4, respectively, for H_2O and NH_3) are the dielectric constants of the Kr and polar molecular films. L_1=32.6 Å is the film thickness for 10 ML Kr and L_2=13.0 and 11.7 Å for 5 ML H_2O and 5 ML NH_3, respectively. In the experiments, the spectra of $A_s(E)$ were measured for 0.1-0.2 ML halogenated molecules (ρ_0 is estimated to be ~6×10^{13}, 5.8×10^{13}, 7.4×10^{13}, 5.0×10^{13} and 1.2×10^{14} /cm^2 for CF_2Cl_2, $CFCl_3$, CHF_2Cl, CH_3CF_2Cl and HCl, respectively) condensed on a 10 ML Kr film with and without the presence of a 5 ML H_2O/NH_3 layer. The latter has properties sufficiently close to the bulk ice, and keeps the experimental error in measured trapping cross section $\sigma(E)$ due to the uncertainty in H_2O/NH_3 thickness (L_2) negligible since $L_1/\varepsilon_1 \gg L_2/\varepsilon_2$ in Eq. (6).

Reproduced in Fig. 8(a) is $A_s(E)$ for 0.1 ML CF_2Cl_2 adsorbed on a 10 ML Kr surface, from which a trapping cross section σ=1.4×10^{-15} cm^2 at nearly 0 eV was derived, which is about 14 times the DEA cross section in the gas phase. As shown in Fig. 8(b), in contrast, a DEA resonance peaking at 0 eV with a cross section of σ=7.2×10^{-15} cm^2 was observed for $CFCl_3$, which is slightly smaller than the gas-phase DEA cross section (~1×10^{-14} cm^2), along with a much weaker peak appearing around 6.0 eV [89]. The larger DEA cross section for CF_2Cl_2 adsorbed on the Kr surface than the gas-phase cross section has been well explained by the

condensed phase effects on the lifetime, decay channels and energy of anion resonances [13], well described in the R-matrix model by Fabrikant [92, 93]. In contrast, the smaller DEA cross section for $CFCl_3$ adsorbed on the Kr surface than its gas-phase DEA cross section at zero eV has been attributed to the reduction in nuclear wave function overlap between the neutral AB and the anion AB^{*-} states in the Franck-Condon region [89].

Of special interest are the results of $A_s(E)$ for 0.1 ML CF_2Cl_2 and $CFCl_3$ condensed on 5ML H_2O predosed onto the 10 ML Kr surface, which are shown in Figs. 8(c) and 8(d), respectively. Evidently, the presence of the polar molecular films leads to a complete quenching of DEA resonances at electron energies larger than ~1.0 eV but increases the electron trapping cross section near 0 eV. However, the trapping coefficient in Figs. 8(c) and 8(d) may include contribution from long-lived electrons trapped in the pure H_2O film [13]. After subtracting the latter, a trapping cross section $\sigma=1.3 \times 10^{-14}$ cm^2 at ~ 0 eV for 0.1 ML CF_2Cl_2 on 5 ML H_2O was obtained, which is about one order of magnitude larger than that on Kr or two orders higher than the gaseous cross section [13]. Similarly, a trapping cross section of ~8.9×10^{-14} at ~ 0 eV for 0.1 ML $CFCl_3$ on 5 ML H_2O was measured, which is nearly one order higher than the gaseous cross section [90].

The results of $A_s(E)$ for 0.1 ML CHF_2Cl (HCFC-22) and 0.1 ML CH_3CF_2Cl (HCFC-142b) adsorbed onto the 10 ML Kr surface from Lu and Sanche [89] are reproduced as Figs. 9(a) and 9(b), respectively. From these $A_s(E)$ values, the DEA cross sections for HCFC-22 and 142b were measured to be ~4.2×10^{-16} cm^2 broadly peaking at 0.78 eV and ~7.8×10^{-16} cm^2 at 0.89 eV, respectively, which are 2 to 3 orders of magnitude larger than their gaseous values. For HCFC-22, there are also two small peaks at 4.7 eV and 8.0 eV. The results of $A_s(E)$ obtained for 0.1 ML CHF_2Cl and 0.1 ML CH_3CF_2Cl adsorbed on 5ML H_2O predosed onto the 10 ML Kr surface

from Lu and Sanche [90] are reproduced in Figs. 9(c) and 9(d), respectively. The measured trapping cross sections at ~ 0 eV are ~5.1×10^{-15} and ~4.9×10^{-15} cm^2 for CHF$_2$Cl and CH$_3$CF$_2$Cl on H$_2$O ice, respectively, which are approximately 3-4 orders of magnitudes larger than their respective values in the gas phase.

Lu and Sanche [88] also measured the A$_s$(E) for HCl adsorbed on 10 ML Kr and on 5ML H$_2$O predosed onto 10 ML Kr, from which electron trapping cross sections $\sigma = (1.1 \pm 0.3) \times 10^{-16}$ and $(4.0 \pm 1.2) \times 10^{-15}$ cm^2 at ~0 eV were derived. Evidently, the presence of H$_2$O greatly increases electron trapping at ~0 eV. Similar DET reaction is expected for ClONO$_2$, though it was not done in the experiments. The reason is that ClONO$_2$ has not only a strong DEA resonance at 0 eV but its dissociation is highly exothermic (by up to 2.1 eV) [94]. Thus, there is every reason to predict that the DET of ClONO$_2$ with electrons trapped in polar ice has the highest efficiency, no less than those of CFCs.

It is also worth noting the following facts. (1) The condensed-phase effects lead to a *decrease* of the DEA cross section at zero eV of CFCl$_3$ (CCl$_4$) adsorbed on a non-polar Kr film. (2) For halogenated molecules (CFCs, HCFCs, HCl, etc.), except electron-trapping cross sections at near 0 eV, the DEA resonances at electron energies ≥1 eV observed in the gas phase and on the Kr surface are almost completely suppressed when they are adsorbed on the ice surface. More significantly for HCFCs, the higher-energy sides of the DEA resonances at electron energies ≥1 eV disappear when these molecules are adsorbed on H$_2$O ice. This is even clearer for CF$_4$, which has a DEA resonance peak around 6.0 eV observed for CF$_4$ adsorbed on the Kr surface by Bass et al. [95], but the resonance completely disappears on the H$_2$O ice surface [90]. These observed results demonstrate that the H$_2$O ice causes a quenching effect on the DEA resonances above 1.0 eV. In striking contrast, the electron trapping cross sections of

these halogenated molecules at 0 eV are greatly enhanced by the presence of the H_2O ice films. It is evident that such enhancements cannot be explained by the above-mentioned condensed phase effects observed for molecules adsorbed on non-polar Kr films. Instead, these results have confirmed the DET mechanism expressed in Eqs. (4) and (5). The excess electrons near 0 eV are rapidly thermalized and trapped in the polar H_2O ice to become weakly-bound pre-solvated electrons (e_{pre}^-). During its lifetime, e_{pre}^- is effectively resonantly transferred to a halogenated molecule that has an anion resonance in the energy range of e_{pre}^- ($-1.5 \sim -1.0$ eV) (Fig. 1). Note that the fully-solvated electrons with a binding energy of 3.2 eV in the H_2O bulk can hardly contribute to the DETs of halogenated molecules, as well demonstrated in the experiments in liquid water [21, 27-29].

Strictly speaking, the above electron trapping measurements could not distinguish whether the electron is trapped as the Cl^- fragment or a stabilized molecular ion (e.g., a $CF_2Cl_2^-$). However, it has been pointed out that even for gaseous CFCs with DEA resonances near 0 eV, the dissociation probability of the AB^{*-} transient state lies near unity once an electron is attached [32]. This is most likely to be true for AB^{*-} states resulting from DETs of halogenated molecules with e_{pre}^- in H_2O, since their autodetachment cannot occur (see Fig. 1) [29]. And desorption of Cl^- from the surface is negligible. Thus, the measured charges are approximately equal to electrons trapped as Cl^- ions, i.e., σ approximately corresponds to the DEA/DET cross section [13, 88-90]. The DET cross section of CF_2Cl_2 on H_2O ice measured in electron trapping experiments is very close to the value estimated from the ESD measurements. Thus, the low-electron trapping experiments at 0-10 eV with an excellent energy resolution (40 meV) provided an ideal complement to the ESD measurements, well confirming the DET mechanism.

C. Femtosecond time-resolved laser spectroscopic measurements

Real-time observation of the reaction transition state is the most direct method for observation of molecular reactions and bond breaks, according to the seminal contributions of Nobel laureates Drs. Polanyi and Zewail [96]. This came true with the advent of femtosecond time-resolved laser spectroscopy, as demonstrated by the pioneering work of Zewail [97]. Using this technique, Wang et al. [21, 27-29] have obtained direct, real-time observations of the intermediate anion states (XdUs*$^-$ and CCl$_4$*$^-$) of the DETs of e$_{pre}^-$ with lifetimes of 200-500 fs to Cl-, Br- and I-containing molecules, namely halopyrimidines (XdUs) and CCl$_4$, in liquid water/methanol. As shown in Fig. 10, the formation time of XdUs*$^-$ just corresponds to the lifetimes of e$_{pre}^-$, which are within 1.0 ps after the electron is generated by a fs laser pulse. These results directly prove that the DET reactions occur with the pre-solvated electron, rather than with the fully solvated electron, a notion held since 1970s.

With a different approach, Ryu et al. [16] and Bertin et al. [17] have also observed the DET reactions of CFCs adsorbed on H$_2$O ice on a metal substrate by monitoring the dynamics of trapped electrons with fs time-resolved two-photon photoemission (2PPE) spectroscopy. As shown in Fig. 11, Ryu et al. [16] showed that the lifetime of an electron photoexcited from a metal substrate and trapped in the ice film is significantly decreased by co-adsorption of submonolayer CFCl$_3$, which was explained by DET of the "solvated" electron from the ice to CFCl$_3$. It should be noted that the transient electron species with a lifetime of 120 fs observed by Ryu et al. is in a weakly-bound state at 1.2 eV below the vacuum level and is a pre-solvated electron rather than a fully solvated electron that has a binding energy of ~3.2 eV [56]. As reproduced in Fig. 12, similar results were recently observed by Bertin et al. [17] for CFCl$_3$ adsorbed on the crystalline ice surface, but they observed long-lived trapped electrons with a

lifetime up to minutes, trapping at pre-existing structural defects on the surface of the crystalline ice. The results of Bertin et al. indicated that DET of the trapped electrons from the ice to $CFCl_3$ is highly efficient, since an extremely low $CFCl_3$ coverage of only ~0.004 monolayer can completely deplete all the trapped electrons generated in the ice under their experimental conditions (Fig. 12). The observations by Bertin et al [17] are interesting, but it should also be noted that such long-lived trapped electrons may not be unique to the crystalline ice surface. Indeed, long-lived trapped electrons were also observed at the amorphous ice film deposited on Kr at 20 K in the electron trapping experiments [13]. The 2 PPE experimental results by Ryu et al. [16] and Bertin et al. [17] also agree with the observations of Lu and Madey [11, 12, 79, 80] that the anionic-yield enhancement factor due to the DET process is strongly dependent on the coverage of CFCs. Bertin et al. [17] also explore the implication of their results for photo-enhanced DET reactions of CFCs in the lower polar stratosphere with the returning of sunlight in spring. However, it should be noted that most of the CFC molecules have been depleted in the lower polar stratosphere during winter, so have HCl and $ClONO_2$ molecules; the concentrations CFCs are very low in spring (see satellite data to be presented in Section V(D)). Nevertheless, it will still be interesting to explore the possible effects of photo-assisted DET reactions of other halogenated molecules (e.g., ClOOCl) on ozone loss in the spring polar stratosphere.

D. Other measurements

There are also other studies of electron induced reactions of condensed CF_2Cl_2 (CCl_4) or the CF_2Cl_2 (CCl_4) / H_2O ice mixtures deposited onto a metal surface [98-103]. However, refs. 98-100 and others not cited here studied the dissociation electron attachments (DEAs) of pure CFCs with free electron energies (0-20 eV) and are therefore beyond the scope of this review. In terms

of the X-ray photoelectron spectroscopy (XPS) and reflection absorption infrared spectroscopy (RAIRS) studies of CCl_4/H_2O and CF_2Cl_2/H_2O ice mixtures on Au by Fairbrother and co-workers in 2002-2003 [101, 102], one has to be discerning in discussing the relevance of their results to the DETs of CFCs adsorbed on H_2O ice. In those studies, secondary electrons from a metal (Au) were generated from a X-ray source (Mg Kα anode, 1253.6 eV) operating at 300 W and 15 kV or from a high-current flood electron gun at 4 mA emission current and a 10 eV extraction voltage. For the latter, a sample bias of +200 V was employed to accelerate the kinetic energy of the incident electrons and increase the rate of chemical transformation in the CCl_4/H_2O (ice) films. Their results showed a slow depletion of CCl_4 or CF_2Cl_2 molecules identified by RAIRS ν(C-Cl) and ν(C-F) peaks, respectively [101, 102]. For instance, about 10% of CF_2Cl_2 remained on the surface with extended exposure of the X-ray source by $\geq$500 min [102]. The secondary electron current generated such a X-ray source is typically in the order of μA. These results implied no or little enhancements or even a decrease in the cross sections of electron-induced reactions of the CFC/ice mixtures compared with the cross sections for pure CFCs. It must be pointed out, however, that the thicknesses of the CCl_4/H_2O and CF_2Cl_2/H_2O films used in their XPS/RAIRS experiments were $\geq$300 Å (~100 ML H_2O) and 60-70 Å (~20-23 ML H_2O), respectively. Under the conditions, secondary electrons generated from the Au substrate could hardly reach all CCl_4/CF_2Cl_2 molecules, and it was not clear if the decomposition of CFCs is dominated by the interaction with high-energy incident electrons / photons or with low-energy secondary electrons. In fact, Fairbrother and co-workers [101] stated that "the same chemical transformations (reaction products) were observed for CCl_4/H_2O (ice) films using the X-ray source or the electron gun in the absence or presence of an applied bias voltage (+200)". If this observation was confirmed, then it would mean that no secondary electrons from the metal

were involved in the chemical transformation. The reason is that the secondary electron yield is well known to be strongly dependent on the incident primary electron energy [104]. Indeed, almost no secondary electron emission from a metal substrate could be observed for an incident primary electron beam of 10 eV [80, 104], and the electron trapping cross section of ice at 10 eV is nearly zero (see Figs. 8 and 9). Thus, when the flood electron gun was operated at 10 eV without applying a bias voltage, essentially no secondary-electron-induced reactions (DEA/DET) could occur at the pure CCl_4 or CF_2Cl_2 layer or in the CCl_4/ice or CF_2Cl_2/ice mixture. Overall, these XPS/RAIRS studies of thick CFC/ice mixture films did not have the capability of obtaining the quantitative DEA/DET cross section of CFCs [101, 102].

In 2004, Fairbrother's group in collaboration with Madey's group [103] also reported their measurements of the DET cross sections of CFCs adsorbed on top of 5 ML H_2O using temperature programmed desorption (TPD). Unfortunately, however, their results were essentially misinterpreted. With energy-undefined, yield-unknown secondary electrons generated by the X-ray source or a defocused 180 eV electron source from a QMS filament, these authors claimed obtained "direct" measurements of the absolute DET cross sections of CCl_4 or CF_2Cl_2 adsorbed on ice. Their measured dissociation rates of 1ML CF_2Cl_2 and 1 ML CCl_4 increased in an H_2O (D_2O) environment by ~2–3 times, which is *not* smaller than that reported in literature [11, 12], as seen in Fig. 4(a). However, the maximum absolute cross sections for decomposition of 0.25 ML CFCs adsorbed on top of 5 ML H_2O, using 180 eV incident electrons from the QMS filament, were measured to be $1.0\pm0.2 \times 10^{-15}$ cm^2 for CF_2Cl_2 and $2.5\pm0.2 \times 10^{-15}$ cm^2 for CCl_4. The latter is even less than the reported DEA cross sections of CCl_4 at 0 eV in the gas phase (1.3×10^{-14} cm^2) [32] and adsorbed on Kr film (5×10^{-15} cm^2) [98]. The authors [103] attempted to compare their measured dissociation cross sections of CCl_4 or

CF_2Cl_2 adsorbed on ice directly with those obtained by Lu and Madey in ESDIAD [11, 12] and by Lu and Sanche in electron trapping experiments [13] reviewed above. Here, a serious and obvious problem must be pointed out: these authors did not take into account the large loss of low-energy secondary electrons in transmission from the metal substrate through 5 ML H_2O to the outmost CFC layer, as robustly seen in the previous experiments by Gilton et al. [77], Chakarov and Kasemo [78] and Lu and Madey [12, see Fig. 5]. According to these previous studies, the tunneling depth of low-energy secondary electrons in H_2O ice is 3-4 ML [77, 78] and the secondary-electron induced dissociation cross section of CF_2Cl_2 (CH_3Cl) adsorbed on top of 5 ML H_2O is about one order of magnitude lower than on 1 ML H_2O [12, 77], as shown in Fig. 5. Thus, the Fairbrother–Madey TPD experiment [103] would have given a maximum dissociation cross section of 1.0×10^{-14} cm^2 for CF_2Cl_2 on 1 ML H_2O ice if the attenuation of secondary electrons in ice were taken into account. This value would then be identical to the cross section of $\sim 1 \times 10^{-14}$ cm^2 measured by ESDIAD of Cl$^-$ from CF_2Cl_2 on 1 ML H_2O ice with 250 eV incident electrons and of 1.3×10^{-14} cm^2 measured by electron trapping with ~ 0 eV electrons incident onto CF_2Cl_2 adsorbed on 5 ML H_2O ice. Obviously, one cannot directly compare the TPD result of CF_2Cl_2 adsorbed on 5 ML H_2O ice using 180 eV incident electrons with the electron trapping result using an incident electron beam reaching 0 eV. But the discrepancy can be removed if the secondary electron flux reacting with CFCs is carefully calibrated in the TPD experiments. However, it was inappropriate for the authors to claim that their TPD gave more "direct" measurements of the absolute DET cross sections of CFCs adsorbed on ice than the ESDIAD directly detecting the desorbing dissociation products (Cl$^-$ and F$^-$) and the electron trapping measurements directly using zero eV incident electrons. In fact, it is the CF_2Cl (mass at 85) and CCl_3 (mass at 117) species, rather than the intact CF_2Cl_2 and CCl_4,

that were detected in the TPD measurements of CF_2Cl_2 and CCl_4 [75, 103]. In a general case, the TPD technique does not have the capability to distinguish the CF_2Cl_2 (CCl_4) and its dissociation product CF_2Cl (CCl_3) adsorbed on the surface.

In summary, there is every reason to conclude that the DET mechanism for halogenated molecules adsorbed on polar molecular ice, originally proposed by Lu and Madey, has been well observed in various laboratory measurements with different methods [11-14, 16, 17, 27-29, 87, 103] and supported by theoretical simulations [105, 106].

IV. SATELLITE OBSERVATIONS OF THE COSMIC-RAY-DRIVEN ELECTRON REACTION MECHANISM

A. Spatial correlation between cosmic rays and ozone depletion

If the CR-driven electron reaction (CRE) mechanism plays a significant role in stratospheric ozone depletion, then a correlation between ozone depletion and the CR intensity should be observed. Due to the geomagnetic effect, the intensity of CRs is well known to be larger at higher latitudes and has a maximum over the South and North Poles, and due to atmospheric ionization, the electron production rate by CRs has a maximum at ~18 km above the ground. Lu and Sanche [14] thus analyzed data of ozone and CRs obtained from field (satellite) measurements and found that there is indeed a strong *spatial* correlation between polar ozone loss and CR intensity in the Earth's atmosphere with variations of latitude and altitude, as shown in Fig. 13(a) and 13(b). The ozone hole is exactly located at the polar stratosphere at ~18 km, where the ionization rate of CRs producing electrons shows a maximum.

B. Time correlation between cosmic rays and ozone depletion

Lu and Sanche [14] also showed a time correlation between the annual mean total O_3 in the southern hemisphere (at latitudes 0–65° S) and the CR intensity in the single CR cycle of 1981-1992. However, it has been argued that no such a correlation would exist beyond one CR cycles [107], or that this time correlation for total ozone in the low and mid-latitudes is only due to the solar effect and no correlation between CRs and O_3 loss in the polar region would exist [108, 109]. It was even argued that no further studies of the CR-driven mechanism for O_3 depletion should be motivated [109]. Facing these criticisms, Lu and co-workers [110, 111] pointed out that the large fluctuation level (up to 20%) of the O_3 data reported in refs. 107-109 did not allow one to examine the effect of the CR intensity modulation (10%) on O_3 depletion over 11-year cycles, as recently demonstrated by Wang et al. [111]. Most recently, Lu [15] has shown that there exist 11-year cyclic time correlations of the CR intensity not only with the annual mean total O_3 in the southern hemisphere (0-60° S) over two CR cycles but with total O_3 in the spring Antarctic ozone hole (60-90° S). The observed data from high-quality ozone datasets of NASA satellites are updated in Figs. 14a and 14b, with the 2008 data included. These observed data have provided strong evidence of the CRE mechanism for the polar ozone hole [15].

C. Direct solar cycle effect and cosmic-ray effect

Atmospheric researchers have attempted to include the so-called solar effect in modeling of the *polar* O_3 loss within the photochemical model, while conceding that it is complicate and difficult to understand the O_3 variation in recent years and predict the future trend [37]. Here, it should be pointed out that this might be a pseudo-problem for at least two reasons. First, the direct solar effect, in inverse phase with the CR effect, argues that the maximum solar UV irradiance

(corresponding to the lowest CR intensity) would result in the maximum O_3 production via the photolysis of O_2 in the upper stratosphere. This effect predicted small annual O_3 oscillations ($\pm 1.5\%$) in the tropics and mid-latitudes but not in the polar region (especially in the lower polar stratosphere) [37]. Second, the photochemical model would also predict that the maximum solar intensity would produce the largest amount of active Cl to destroy O_3.

Researchers have also proposed the direct cosmic ray effect, which attributes ozone loss to the odd hydrogen (HO_x) and odd nitrogen (NO_y) species generated by CRs in the polar stratosphere [112], similar to the production of NO_y species from solar particle events proposed by Crutzen [113]. The direct CR effect would predict an 11-year cyclic variation of total O_3 in the polar stratosphere *in any season*. There may exist other effects of charged particle precipitation on O_3 loss in the upper stratosphere [37]. However, solar particle events and energetic electron precipitation are spontaneous frequent events without an 11-year cycle. Thus, they have been ruled out as the possible mechanisms for the observed 11-year cyclic oscillation in total O_3 [15].

Even without the above reasoning, a direct way to examine the direct solar-cycle and CR-cycle effects is to show the results of time-series total ozone in the summer polar stratosphere: both effects would be most significant to be seen if they exist, while the CRE mechanism is not effective due to the absence of PSCs.

D. Cosmic rays, PSCs and polar stratospheric temperature

There is also strong interest in studying the effects of CRs on cloud cover at low troposphere ($\leq 3km$) and PSCs in the lower polar stratosphere, following the first report of the correlation between CRs and cloud cover by Svensmark and Friis-Christensen [114]. There are a number of

observational studies and model simulations to investigate the physical mechanism for the correlation [115, 116]. The CR-cloud correlation has been reviewed by Carslaw et al. [117]. Since then, other researchers have reported both positive [118] and negative [119, 120] results about the correlation. Similarly, researchers have also studied the possible effects of CRs on the formation of PSCs [121, 122]. One modeling study indicated that strong solar proton events may significantly enhance the formation of large nitric acid trihydrate particles and denitrification [121], while the other showed that "moderate" (May 1990) but not stronger solar proton events may increase aerosol content significantly and cause ozone "mini-hole" creation [122]. Most recently, simulations by Pierce and Adams [123] showed that changes in cloud condensation nuclei concentrations from changes in CRs during a CR cycle are two orders of magnitude too small to account for the observed changes in cloud properties. They hence concluded that the CR-cloud effect is too small to play a significant role in current climate change [123]. In contrast, Svensmark et al. [124] showed the correlation between CRs and atmospheric aerosols and clouds. Overall, the direct CR-cloud (PSC) correlation remains the subject of significant controversies.

It should be emphasized that apart from the direct effects of CRs on PSCs, the decrease in amount of atmospheric ozone can cause significant climatic effects [125-127]. Less ozone in the stratosphere implies less absorption of solar and infra-red radiation there and hence a cooler stratosphere. Thus, significant ozone loss in the spring polar stratosphere has a feedback on the temperature there, which could in turn affect the PSC formation. Ramaswamy et al. [127] reported the stratospheric cooling effect over 1979-2003, where the non-monotonic decrease in lower stratospheric temperature was attributed to the effect of volcanic eruptions. So far,

however, no long-term time correlation between CR intensity and polar stratospheric temperature during any 11-year cycle has been reported.

V. NEW OBSERVATIONS

In spite of the laboratory measurements and observations summarized in Sections III and IV, one might still argue that the other effects mentioned above (solar effect, direct CR effect, and PSCs) might be responsible for the observed correlations between CR intensity and polar ozone loss. Alternatively, one might argue that that the variations of total column ozone measured by satellites might not reflect the real ozone loss caused by ozone-depleting reactions. To make a clear case, 3-month mean total ozone data in the *summer* and *spring* polar area from both NASA satellites and BAS ground-station measurements over Antarctica in the period of 1979 to 2008 are presented and all possible mechanisms are discussed below. Furthermore, the time-series polar stratospheric cooling as a result of O_3 loss at an Antarctic station (Halley) from 1956 to 2008 (over 50 years) is also presented. These observations not only provide an important examination of the time correlation between polar O_3 loss and CR intensity but show the significant impacts of CFCs and CRE-driven ozone depletion on stratospheric climate change. Moreover, the seasonal variations of CFCs and so-called trace gases (N_2O and CH_4) in the polar stratosphere will also be presented and discussed.

A. Comparison between observed data with photochemical model

Due to the Montreal Protocol, the total halogen level in the lower atmosphere was measured to peak in 1994 and the equivalent effective stratospheric chlorine (EESC) over the Antarctica was estimated to peak around 2000 with a given delay of 6($\pm$3) years [37]. To reduce the O_3 data

uncertainty, the time series 3-month average zonal-mean total O_3 variations in the polar stratosphere at latitudes (60°-90° S) in the months of the Antarctic ozone hole, namely October, November and December from 1979-2008, obtained from NASA TOMS satellite (N7, M3, EP and OMI) datasets, are presented here. Note that most of the daily average ozone data in September in the NASA satellite datasets only cover the latitudes (0-80° S) and the September monthly average ozone data are therefore not included. As shown in Fig. 15(a), the 3-month average O_3 data have a much lower fluctuation level than the October monthly data shown in Fig. 14 [15]. The data show that the Antarctic O_3 decreased drastically from the end of 1970s to 1990, following the significant rise of the halogen loading in the stratosphere. The large El Chichón volcanic eruption in 1982 ejected a large amount of sulfur gases into the stratosphere, leading to unusually large fluctuations of the O_3 data in 1980s. From 1990 to the present, the polar total O_3 has clearly exhibited a cyclic oscillation with a periodicity of 11 years. In contrast, the O_3 results predicted by the photochemical model simulations are shown in Fig. 15(b), which predict that the Antarctic springtime O_3 would recover (increase) by 5% to 10% between 2000 and 2020 [37]. This prediction is clearly inconsistent with the observed data. More evidently, several photochemical modeling calculations have predicted a *minimum* Antarctic ozone hole in 2008-2009, which is exactly opposite to the observed fact. In fact, essentially no changes in the stratospheric O_3 layer over the Equator, where sunlight is the strongest, have been observed over the past decades (Fig. 13(a)).

B. **Confirmation of the 11-year cyclic ozone loss over spring Antarctica**

Fig. 16(a) plots the time series variations of both CR intensity and the 3-month average zonal-mean total O_3 in the springtime Antarctic stratosphere (60°-90° S) over 1979 to 2008 from

NASA satellite datasets. Indeed, the springtime O_3 loss data clearly exhibit a pronounced time correlation with the CR intensity variation over the 11-year cycles from 1990s (more precisely from 1995) up to the present. Although the NASA satellite data have been widely used in ozone research, it might as well show other measured data sources. Thus, time series 3-month (September-November) mean springtime ozone data obtained from the Antarctic ground-station measurements at Halley (75°35'S, 26°36'W) from 1979-2008 are shown in Fig. 16(b). A quite similar 11-year cyclic variation of the springtime ozone at the Antarctic station from 1995 up to the present is again observed. Thus, these data now clearly establish that the ozone loss in the Antarctic hole indeed shows an 11-year cyclic variation following the oscillation of the CR intensity. From 1995 up to the present, the variation of the EESC in the polar stratosphere has been much milder, passing the plateau (Fig. 15(a)). Thus, the total ozone oscillation caused by the variations of CR intensity has become most pronounced.

Fig. 16(c) shows the available 2-month average zonal mean O_3 in the *summer* Antarctic stratosphere (60°-90° S) and 3-month (January-March) mean *summer* ozone data at Halley over 1979 to 2008. In striking contrast to the spring (Oct-Dec or Sept-Nov) total ozone, no such time correlation exists between the zonal-mean total O_3 in the summer polar stratosphere and the CR intensity variation. *These observed data clearly rule out both the solar cycle effect and the direct CR effect responsible for the observed 11-year cyclic total ozone variation.*

As a matter of fact, the observation of pronounced 11-year cyclic oscillations of the total O_3 in the polar ozone hole has forced one to conclude that the CR-driven mechanism must play a dominant role in the polar zone loss [15]. The reason is that the oscillation amplitude of the CR intensity in the 11-year CR cycles is well-known to be only ~10% of its median, so that the

oscillation amplitude of the resulting polar ozone loss would be too small to observe, unless the CR-driven mechanism play the dominant role.

C. Observation of 11-year cyclic stratospheric cooling due to ozone loss

To distinguish the temperature variations induced directly by CRs and indirectly by the CR-driven O_3 loss and to show if the decrease in total O_3 reflects real chemical O_3 loss, the temperatures at the lower Antarctic stratosphere (100 hPa) at Halley during the winters (June-August, prior to the Antarctic O_3 hole season), the later springs (November, after the O_3 hole peak) and the annuals over the past 50 years (1956-2008) are shown in Fig. 17. As shown in Fig. 17(a), the winter polar stratospheric temperature does not show a pronounced oscillation over 11-year CR cycles. In contrast, Fig. 17(b) shows that the polar stratospheric temperature in November (just after the ozone-hole peak) exactly follows the total ozone there, *showing strong 11-year cyclic variations.* These strong oscillations are conveyed into the weaker oscillations in annual mean polar total ozone and temperatures, as shown in Fig. 17(c). Note that the temperature in the polar stratosphere prior to the ozone-hole season shows no significant time correlation with the CR/solar intensity variation (Fig. 17a). This observation demonstrates that neither the solar cycle effect nor the pure CR effect (without involving ozone loss) is responsible for the present observation of 11-year cyclic stratospheric cooling.

Moreover, it is strikingly shown in the Fig. 18 that the lower stratospheric temperatures over the Halley station in November and annual exhibit excellent linear dependences on total ozone there over the past 50 and 30 years, respectively. Even the linear fits give very high correlation coefficients R=0.94 and R=0.89, respectively, with the probability (that R is zero) P<0.0001. These data (Figs. 17 and 18) clearly demonstrate that the long-term temperature change in the

lower polar stratosphere is solely dependent on the variation of total ozone; both exhibit pronounced 11-year cyclic variations. This is clearly in contrast to the previous attribution of the non-monotonic decrease in the stratospheric temperature to the effect of volcanic eruptions [127] or to the effects of non-CFC greenhouse gases [37]. The present observations provide strong evidence that the CRE-driven polar ozone loss results in a subsequent 11-year cyclic stratospheric cooling. The stratospheric cooling will affect the polar stratospheric temperature and associated formation of PSCs in the subsequent year. This could cause a feedback effect on ozone depletion, as shown in the CRE modeling described in Section VI.

D. Seasonal variations of CFCs, N₂O and CH₄

In current content of atmospheric chemistry, "air descending" is attributed to be responsible for the concentration decreases of CFCs and some photo-inactive "tracer" gases such as N_2O and CH_4, and thus any physical/chemical processes for CFCs are excluded for the *winter* polar stratosphere [37, 128]. However, two major problems with this assignment must be addressed. First, one must make sure whether DEA/DET processes could occur for these so-called "trace" molecules and whether the radicals resulted from the DEA/DET reactions of CFCs could react with these "trace" molecules. For example, N_2O has been used as the standard "trace" gas in atmospheric chemistry because it is photo-inactive. *This assignment would be valid only if there were no physical or chemical processes leading to the loss of N_2O in the polar stratosphere*. Unfortunately, just similar to CFCs, N_2O is well-known to have strong DEA resonances at low electron energies at 0.6 and 2.3 eV with an energy threshold of 0.21 eV in the gas phase [129, 130]. The later is expected to be −1.1 eV on the surface of H_2O ice due to the polarization potential of ~1.3 eV [30], and hence DET should occur for N_2O on ice. Indeed, there is solid

evidence that DET of N_2O can effectively occur with weakly bound electrons, e.g., photoexcited subvacuum hot electrons [131], electrons from Cs-covered surfaces with work-functions of 1.7-2.2 eV [132] or photoassisted Li atoms in the Li-N_2O complex [133]. Even the latter study showed the reaction of CH_4 with O^- or $O(^1D)$ resulted from the DET of N_2O, and similar reactions might also occur with the DET products of chlorine-containing molecules (CFCs). Nevertheless, it should also be noted that DET of weakly-bound electrons in PSC ice with CH_4 itself is not expected to occur since CH_4 does not have a DEA resonance at low electron energies below 5 eV in the gas phase [134]. Thus, CH_4 might be a better "trace" gas than N_2O, though its absolute inertness is not guaranteed for the above reason.

Second, the "compact" CFC-N_2O correlation from the satellite or balloon data taken in September has been used to support the photochemical model of ozone depletion. However, one should note that September is *in spring (rather than in winter)*, when the O_3 hole has formed. The result cannot be taken as the valid evidence to exclude the CR-driven electron reactions of halogenated molecules in the polar stratosphere *in winter*. Here, the observed monthly average CH_4 data combining the data from both the Cryogenic Limb Array Etalon Spectrometer (CLAES) and Halogen Occultation Experiment (HALOE) aboard the NASA Upper Atmosphere Research Satellite (UARS) and spanning over the winters of 1992–1998, and the CF_2Cl_2 data over the winter of 1992 from the CLAES are shown in Fig. 19. It can be clearly seen that until the end of winter (August), the CH_4 level significantly dropped at the higher polar stratosphere above 20 km, but this did *not* occur in the *lower* Antarctic stratosphere *below 20 km*. This is contrast to the CF_2Cl_2 level that decreased from ~320 in April to 200 pptv in August and 160 pptv in September. These data indicate that DET reactions of CFCs must have occurred in the winter lower polar stratosphere where and when there is no sunlight. Just like stratospheric

cooling (Fig. 17), air descending (the CH_4 level drop) in the *lower* polar stratosphere below 20 km *in spring* is a consequence, rather than a cause, of the spring ozone hole.

Atmospheric chemists have concerns about how CFCs and other halogenated molecules could be adsorbed on ice particles in PSCs [128]. However, it is known to surface scientists that although CFCs are not sticky to the *static* surfaces of H_2O ice at the stratospheric temperature under the vacuum condition, dynamical and other physical properties of ice surfaces under polar stratospheric conditions can make a drastic difference, causing adsorption, diffusion and trapping of molecules into ice. This subject was reviewed recently by Girardet and Toubin [135]. Experimental studies [136, 137] showed that the interactions of CF_2Cl_2 molecules with crystalline and amorphous water films are rather complicated. Most recently, Souda [137] concluded that the interactions of CF_2Cl_2 with ice surfaces are significantly different from that with an inert (static) graphite substrate; CF_2Cl_2 molecules do not simply physisorb on the surface of ice and might be incorporated into the bulk of the amorphous ice film at temperatures ≥ 57 K. Further laboratory studies on the adsorption, diffusion and trapping of CFCs at ice surfaces under the polar stratospheric conditions seem necessary.

VI. TOWARDS QUANTITATIVE UNDERSTANDING OF OZONE DEPLETION

The CRE mechanism states that in the winter polar stratosphere, the O_3-depleting reactions depend on halogen concentrations (EESC), the intensity I of CRs to produce electrons and the amount of PSCs to trap the electrons [14, 15]. Thus, the CRE mechanism, taking the stratospheric cooling caused by the preceding-year polar ozone loss into account, gives the steady-state total ozone ($[O_3]_i$) in the Antarctic in a particular period in spring (*i*) as:

$$[O_3]_i = [O_3]_0[1 - k \times I_i \times I_{i-1} \times EESC_i], \tag{7}$$

where $[O_3]_0$ is the total ozone in the polar stratosphere when *EESC=0* ($\approx$310 and 375 DU for the

October and 3-month (Oct-Dec) average zonal mean total O_3), I_i the CR intensity in the *i*th year

and *k* a constant. In Eq. (7), it is simply assumed that *the photolysis of halogens in the spring*

polar stratosphere is not a limiting factor. With the measured CR intensities, it is strikingly

shown in Figs. 16(a), 16(b), 17(b) and 17(c) that Eq. (7) gives good fits to the observed ozone

data from 1950s to 2008. Indeed, we can see that the CRE model gives the maximum O_3 losses

in 1987 and 1998, in agreement with the observed data. Remarkably, the simplified CRE model

expressed in Eq. (7) is by no means aimed to give a precise calculation of total ozone in the polar

stratosphere, but rather to give an approximate envelope of the long-term total ozone change.

Surprizingly, the fitted results demonstrate that the CRE model as the sole mechanism can

reproduce the observed data pretty well. In the earlier paper [15], a linear dependence of

monthly average zonal-mean total O_3 on the CR intensity from 1990-2007 was fitted. But there

were severe limitations to the linear fitting: it could only give a poor fit to the observed data in a

short period of time (from 1990-2007), and could not give a good fit to the whole spectrum of

the observed data, particularly in the drastic O_3-decreasing period of 1979-1990. This is

drastically different from the nearly quadratic dependence revealed in Eq. (7), which can now

give fairly good fits to all the observed data from 1950s to 2008.

VII. FUTURE TREND OF THE OZONE HOLE

The intensity of cosmic rays is still peaking in 2009, so we should expect to observe one of the

deepest ozone holes over the spring Antarctica in 2009~2010. With the measured I_{08}=10132 for

2008, Eq.(7) gives the total ozone ratio $[O_3]_{08}/[O_3]_0$=59.2% in the spring Antarctic ozone hole, which is very close to the observed value of 60.6% for 3-month (October-December) average zonal-mean total ozone over the Antarctica (60-90° S) from NASA OMI satellite. With I_{09}=10455 as of June 30, 2009, Eq.(7) predicts a variation $[O_3]_{09}/[O_3]_0 \approx$58.5% for the total O_3 in the spring Antarctic ozone hole in 2009. This value is therefore predicted to be nearly identical to the lowest record of $[O_3]_{98}/[O_3]_0$=58.7% observed in 1998. Similarly, the CRE model will predict the 3-month (October-December) average zonal-mean total O_3 values over the Antarctica (60-90° S) in 2009 to be 219±5 DU. Note that although the 2006 Antarctic ozone hole made a record of ~181 DU in the October average zonal-mean total O_3, the observed 3-month average zonal-mean total O_3 in 2006 was ~225 DU, lightly larger than ~220 DU observed in 1998 in the NASA TOMS satellite data. Thus, we expect to see one of the deepest O_3 holes in spring 2009, which may also occur for spring 2010, depending on the CR-intensity variation and polar meteorological conditions.

With the CRE mechanism, one should be able to predict the future trend of the ozone hole. The intensity variation of CRs with an average periodicity of 11 years and its oscillation amplitude of ~10% are well known. Thus, the time series CR intensity can be expressed as

$$I_i = I_{i0}\left\{1+10\%\sin[\frac{2\pi}{11}(i-i_0)]\right\}, \tag{8}$$

where I_{i0} is the median CR intensity in an 11-year cycle. Note that I_{i0} in recent CR cycles has an increasing rate of ~2% per 11-year cycle. As shown in Fig. 20(a), the best fit to all the CR data observed at the Antarctica (McMurdo) from 1960s-2009 yields I_{i0}=8800[1+2%(i-1979)/11]. The

– 41 –

estimated EESC data for the future are available from the WMO Report [37], as shown in Fig. 20(b). The theoretical results of total O_3 in the spring Antarctic stratosphere for 1979-2060 given by Eqs. (7) and (8), with respect to $[O_3]_0$, are shown in Fig. 20(c). Interestingly, the calculated data agree very well with the observed data, and a clear cyclic variation of O_3 loss in the Antarctic hole is predicted. The CRE model predicts another deepest O_3 hole around 2020, as shown in Fig. 20(c). Although atmospheric dynamics and meteorological conditions could cause large total O_3 fluctuations from year to year [37], a long-term trend of the polar O_3 loss is predictable.

The future trend of the O_3 hole will depends on not only the halogen loading in the stratosphere but the variation of CRs. According to the CRE mechanism expressed in Eq. (7), the depletion of total ozone has a nearly *quadratic* dependence on the CR intensity I_i. If the mean CR intensity keeps the same variation trend as in the past three CR cycles from 1965 to the present and the EESC follows the decreasing trend currently projected by recent WMO Report [37], then there will still be total ozone loss of approximately 25% by 2065 even when the EESC drops to the 1980 value and of ~15% by 2100. This means that the complete recovery of the Antarctic O_3 hole would not occur even by the end of this century. This estimation certainly depends on the variation trends of the CR intensity and stratospheric halogen concentrations.

VIII. EFFECTS OF CFCS AND CRE-DRIVEN OZONE DEPLETION ON GLOBAL CLIMATE CHANGE

It is also interesting to note that CFCs and CRE-driven stratospheric ozone depletion can have significant effects on not only stratospheric but global climate [138, 139]. There are two opposing effects of stratospheric ozone loss: it causes less absorption of solar radiation there and

hence a cooler stratosphere but a warmer troposphere; the resulting colder stratosphere emits less long-wave radiation downward, thus cooling the troposphere. It has been concluded that overall, the cooling effect of ozone depletion dominates. The observed stratospheric ozone depletion over the past two decades has caused a negative forcing of the surface-troposphere system of about -0.15 ± 0.10 W/m² [139]. Moreover, ozone-depleting molecules (particularly CFCs) themselves are also well-known greenhouse gases [138, 139]. The IPCC concludes that the increases in concentrations of these chemicals have produced 0.33 ± 0.03 W/m² of radiative forcing, representing about 13% of the total radiative forcing from increases in the concentrations of well-mixed greenhouse gases [139]. *However, these conclusions were based on climate model simulations, rather than direct observations.* Thus, direct observations of the effects of CFCs and CR-driven ozone depletion on global climate may have far-reaching significance.

Although the IPCC has concluded that CO_2 is major culprit for surface global warming, it is still the subject of great controversies. The data shown in Figs 17 and 18 indicate that CFCs and CRE-driven ozone depletion strongly affect the climate in the polar region, while non-CFC greenhouse gases play a negligible role. Furthermore, the severe polar ozone depletion also substantially affects global ozone (60°S-60°N), especially in the mid-latitudes, where the air mixes more readily with ozone-depleted air from the poles. The extent of the contribution of polar ozone depletion to midlatitude ozone depletion is estimated to be about one-third in the Northern Hemisphere and one-half in the Southern Hemisphere [37]. The larger contribution in the Southern Hemisphere is due to the larger polar ozone depletion in the Antarctic relative to the Arctic region. At present, the globe stratospheric ozone is about 4% below the pre-1980 average, while total ozone loss has reached 3% in the Northern Hemisphere and around 6% in

the Southern Hemisphere since 1980 [37]. Although a few percent depletion of global stratospheric ozone may have a limited effect on global surface temperature, CFCs are well-known effective greenhouse gases [138, 139]. It is therefore significant to have more careful studies of the effects of CFCs and CRE-driven ozone depletion on global climate. For this purpose, the southern hemisphere (SH), northern hemisphere (NH) and global surface temperatures are plotted together with the EESC from 1850 to 2009 in Fig. 21. The EESC data prior to 1970 were not measured [37] and were hence calculated by extrapolating the observed data of 1970-1980, assuming an identical growth rate. Strikingly, it is shown that except the short-period large fluctuations, the SH, NH and global surface temperatures did not rise appreciably (within 0.1 ^{o}C) from 1850 to 1950, during which period CO_2 was the dominant greenhouse gas and increased linearly. In contrast, all of the surface temperatures started to increase around 1950, when the EESC started to be significant. Since then, the surface temperatures closely followed the variation trend of the EESC and increased by ~0.15 ^{o}C/decade from 1950 to 2002~2005. Remarkably, the EESC has been estimated to peak in the stratosphere around 2000 by assuming a delay Γof 6 years with a width of 3 years from the peak in 1994 measured at the surface [37]. Correspondingly, the observed SH, NH, global surface temperatures have a turnover in 2002, 2005 and 2005, respectively, and have clearly decreased by 0.22, 0.15 and 0.16 ^{o}C to 2008, respectively. In contrast, the CO_2 level has kept increasing with the highest rate [139]. Most strikingly, it is found that the observed global surface temperature variations ΔT (relative to the 1980 value) have an excellent linear dependence on the EESC values (normalized to the 1980 value), as shown in Fig. 22(a). A relationship, ΔT=−0.31+0.30×EESC (^{o}C) with a correlation coefficient R as high as 0.89 and the probability (R=0) P<0.0001, is obtained from the linear fit. As shown in Fig. 22(b), moreover, the time-

series data also exhibit weak but visible 11-year cyclic oscillations in the surface temperatures, following the 11-year CR cycles. *These data strongly indicate that global temperature has been dominantly controlled by the level of CFCs, modulated by the CR-driven ozone depletion over the past century.* There are two reasons for the observed faster SH temperature drops since 2002. First, the greenhouse effect of CFCs decreases due to the drops of CFC concentrations in the stratosphere. Second, the observed enlarged ozone depletion in the Antarctic stratosphere from 2002 up to the present due to the rising CR intensity [15] has led to enhanced cooling in the surface. Both effects could lead to the rapid surface temperature decrease. The observed data from 1850 up to the present, as shown in Figs. 21 and 22, seem to indicate that CFCs conspired with CRs are the major culprits for not only atmospheric ozone depletion but global warming. The CRE-driven ozone depletion is expected to decrease after 2010 due to the CR cycles, but the EESC will keep decreasing, as shown in Fig. 22(b). If the above observation is confirmed, then we expect to observe a continued decrease in global surface temperature—"global cooling". That is, global warming observed in the late 20th century may be reversed with the coming decades. Indeed, global cooling may have started since 2002, based on the observed data shown in Figs. 21 and 22. This could be very important to the Earth and humans in the 21st century. It certainly deserves for further examinations and studies.

IX. CONCLUSIONS

Laboratory measurements have well demonstrated that electrons can effectively be trapped at ice surfaces and greatly enhance dissociative-electron-transfer reactions of halogenated species (inorganic and organic) adsorbed on the surfaces by orders of magnitude, compared with corresponding gas-phase reactions. The experimental findings summarized in this study have

demonstrated three important features associated with these DET reactions: (1) ultrafast resonant DET reactions of molecules with weakly-bound trapped electrons can occur; (2) the capture probability of electrons by the molecules can be greatly enhanced due to the much longer residence (life) times of electrons trapped in polar media than those of free electrons in the gas phase and quasi-free electrons in non-polar media; and (3) once formed, the autodetachment of the AB^{*-} transient state cannot occur, enhancing its dissociation probability. It has become clear that these features lead to highly efficient DET reactions of halogenated molecules on ice.

It is a robust fact that there is the maximum ionization rate of cosmic rays to produce electrons in the lower polar stratosphere at ~18 km, where ice particles in PSCs are well-known to present in winter. And it is also well-known that CFCs and other halogenated molecules (HCl, $ClONO_2$, etc.) have high concentrations in the lower polar stratosphere in the beginning of winter, which were observed to decrease greatly by the end of winter. A careful analysis of the concentration variations of these halogenated molecules and CH_4 over the seasons from the fall to the spring indicates that the drops of these halogenated molecules in the *winter* polar stratosphere *below 20 km* cannot be attributed to "air descending", which actually becomes significant only after the ozone hole has been formed in spring. Moreover, the observed ozone data do not agree with the predictions from the standard photochemical models (Fig. 15). Since it is dark (there is no sunlight) in the winter lower polar stratosphere and heterogeneous chemical reactions cannot occur for CFCs and HCFCs on ice surfaces, it seems that the CR-driven dissociative electron transfer reaction is the only mechanism for the reactions of these molecules in the winter lower polar stratosphere at altitudes below 20 km, where the ozone hole evolves in the spring. Although heterogeneous chemical reactions of $ClONO_2$ with HCl on PSC ice are not

ruled out in the CRE model, the CR-driven dissociative-electron-transfer reaction of $ClONO_2$ is expected to be highly efficient, no less than those of CFCs, HCl and HCFCs.

Strong *spatial* and *time* correlations between CR intensity and polar ozone loss have now been clearly established, and both the direct solar effect and the pure CR effect have been ruled out for these correlations. Quantitative analyses of the 3-month average zonal mean ozone in the springtime polar area from both NASA satellites and ground-station measurements over Antarctica in the period of 1979 to 2008 have provided a reasonable proof of the CRE mechanism. A simplified equation derived by the CRE mechanism reproduces not only an 11-year cyclic variation of ozone loss but a similar cyclic stratospheric cooling in the polar lower stratosphere from 1956 to 2008. These observed data do not agree with the predictions of the standard photochemical model [37]. Without doubts, atmospheric dynamics and meteorological conditions could influence the CRE-induced reactions and lead to significant fluctuations of total ozone in the polar ozone hole in some years. However, it is reasonable to conclude that the CR-driven DET is the dominant mechanism for activation of photo-inactive halogenated molecules into reactive halogens in the *winter* lower polar stratosphere. And the observed satellite data have demonstrated that the CRE mechanism plays the dominant role in forming the ozone hole in the spring polar stratosphere.

Due to the increasing trend of the CR intensity, the recovery of the ozone hole may be significantly delayed; the full recovery might not occur even by the end of this century. The observations summarized in this study seem to indicate that researchers have to reconsider our understanding of the formation of the Antarctic ozone hole. Mounting observations should allow researchers to reach a consensus on the CRE model in the near future.

Moreover, this review has also shown that CRE-driven polar O_3 loss leads to an 11-year cyclic stratospheric cooling over the past 50 years. The observed data demonstrate that the long-term change of polar stratospheric temperature over Antarctica depends solely on the variation of total ozone, indicating that the effect of greenhouse gases plays a negligible role in the stratospheric cooling over the past five decades. Most strikingly, it is also found that global surface temperature change has an excellent linear dependence on the equivalent effective stratospheric chlorine (EESC). And weak but visible 11-year cyclic oscillations in the surface temperatures are also observed to follow the 11-year CR cycles. These observed data point to the possibility that the global warming observed in the late 20th century was dominantly caused by CFCs, modulated by CRE-driven ozone depletion. With the decreasing emission of CFCs into atmosphere, global cooling may have started since 2002. These observations imply that current climate models may underestimate the effects of CFCs and would have to be revised seriously. This is likely a subject deserving to look at closely.

Finally, the DET mechanism addressed in this study may have fundamental and practical significance in many multidisciplinary areas, no limit to the applications in biotechnology, e.g., for the analysis of human milk triacylglycerols [81] human blood [82] and proteins [140], in disposal of environmentally hazardous halogenated materials [84, 85], and in the activation of anticancer drugs [21-23] and the fundamental understandings of molecular pathways leading to DNA damage and cell death relevant to aging, stroke and cancer and their treatments [24]. For instance, it was recently found by Lu [23] that the DET reaction of cisplatin—the most widely used drug for cancer treatment—with prehydrated electrons generated in a biological environment can greatly enhance the therapeutic efficacy of cisplatin in combination with ionizing radiation. The DET mechanism reviewed in this study sheds light on the principle for

these applications. Furthermore, the DET reaction mechanism involving electron trapping in polar media (particularly H_2O) may have far-reaching significance in biological and environmental systems, in which water is the major constituent.

REFERENCES

[1] R. A. Marcus, Rev. Mod. Phys. 65 (1993) 599 (Nobel Lecture).

[2] A. M. Kuznetsov, *Charge Transfer in Physics, Chemistry and Biology* (OPA, Amsterdam B.V., 1995).

[3] X. Y. Zhu, Ann. Rev. Phys. Chem. 53 (2002) 221; C. D. Lindstrom and X. Y. Zhu, Chem. Rev. 106 (2006) 4281.

[4] S. Larsson, J. Am. Chem. Soc. 103 (1981) 4034.

[5] R. E. Johnson, *Energetic Charge-Particles Interactions with Atmospheres and Surfaces*, Physics and Chemistry in Space Planetology, Vol. 19 (Springer-Verlag, Berlin, 1990).

[6] A. Chutjian, A. Garscadden and J. M. Wadehra, Phys. Report 264 (1996) 393.

[7] B. M. Nestmann, S. V. K. Kumar and S. D. Peyerimhoff, Phys. Rev. A 71 (2005) 012705.

[8] R. N. Compton, in *The role of Rydberg States in Spectroscopy and Photochemistry*, edited by C. Sándorfy, (Kluwer Academic Publishers, Netherlands, 1999) p419.

[9] St.-J. Dixon-Warren, E. T. Jensen and J. C. Polanyi, Phys. Rev. Lett. 67 (1991) 2395.

[10] St.-J. Dixon-Warren, E. T. Jensen and J. C. Polanyi, J. Chem. Phys. 98 (1993) 5938.

[11] Q.-B. Lu and T. E. Madey, Phys. Rev. Lett. 82 (1999) 4122.

[12] Q.-B. Lu and T. E. Madey, J. Chem. Phys.111 (1999) 2861.

[13] Q.-B. Lu and L. Sanche, Phys. Rev. B63 (2001) 153403.

[14] Q.-B. Lu and L. Sanche, Phys. Rev. Lett. 87 (2001) 078501.

[15] Q.-B. Lu, Phys. Rev. Lett. 102 (2009) 118501.

[16] S. Ryu, J. Chang, H. Kwon and S. K. Kim, J. Am. Chem. Soc. 128 (2006) 3500.

[17] M. Bertin, M. Meyer, J. Stähler, C. Gahl, M. Wolf and U. Bovensiepen, Faraday Discuss. 141 (2009) 293.

[18] N. Camillone, K. A. Khan, J. A. Yarmoff and R. M. Osgood, Phys. Rev. Lett. 87 (2001) 056101.

[19] P. Y. Cheng, D. P. Zhong and A. H. Zewail, J. Chem. Phys. 103 (1995) 5153.

[20] D. P. Zhong and A. H. Zewail, Proc. Natl. Acad. Sci. USA 96 (1999) 2602.

[21] C.-R. Wang and Q.-B. Lu, Angew. Chem. Intl. Ed. 46 (2007) 6316.

[22] Q.-B. Lu, S. Kalantari and C.-R. Wang, Mol. Pharmaceutics 4 (2007) 624.

[23] Q.-B. Lu, J. Med. Chem. 50 (2007) 2601.

[24] C.-R.Wang, J. Nguyen and Q.-B. Lu, J. Am. Chem. Soc. 131 (2009) 11320.

[25] G. J. Schulz, Rev. Mod. Phys. 45 (1973) 423.

[26] L. Sanche, Scanning Micros. 9 (1995) 619.

[27] C.-R. Wang, A. Hu and Q.-B. Lu, J. Chem. Phys. 124 (2006) 241102.

[28] C. R. Wang, T. Luo and Q.-B. Lu, Phys. Chem. Chem. Phys. 10 (2008) 4463.

[29] C.-R. Wang, K. Drew, T. Luo, M.-J. Lu and Q.-B. Lu, J. Chem. Phys. 128 (2008) 041102.

[30] Q.-B. Lu, A. D. Bass and L. Sanche, Phys. Rev. Lett. 88 (2002) 147601.

[31] L. G. Christophorou, D.L. McCorkle and A. A. Christodoulides, *in Electron-Molecule Interactions and Their Applications*, Edited by L. G. Christophorou, Vol. 1 (Academic Press, Orlando,1984), chap. 6.

[32] E. Illenberger, H.-U. Scheunemann and H. Baumgärtel, Ber. Bunsenges. Physik. Chem. 82 (1978) 1154; Chem. Phys. 37 (1979) 21.

[33] S. D. Peyerimhoff and R. J. Buenker, Chem. Phys. Lett. 65 (1979) 434.

[34] M. Lewerenz, B. Nestmann, P. J. Bruna and S. D. Peyerimhoff, J. Mol. Struct. 123 (1985) 329.

[35] D. Smith and N. G. Adams, Top. Curr. Chem. 89 (1980) 1.

[36] D. G. Torr, in *The Photochemistry of Atmospheres,* Edited by J. S. Levine, (Academic Press, Orlando,1985), chap. 5.

[37] World Meteorological Organization (*WMO) Scientific Assessment of Ozone Depletion: 2006*, (Global Ozone Research and Monitoring Project-Report No. 50, Geneva, Switzerland, 2007).

[38] C. T. McElroy and P. F. Fogal, Atmos.-Ocean 46 (2008) 15.

[39] E. Dupuy, K. A. Walker, J. Kar, C. D. Boone, C. T. McElroy, P. F. Bernath, et al., Atmos. Chem. Phys. 9 (2009) 287.

[40] M. J. Molina and F. S. Rowland, Nature 249 (1974) 810.

[41] P. J. Crutzen, J. Geophys. Res. 30 (1971) 7311.

[42] J. C. Farman, B. G. Gardiner, and J. D. Shanklin, Nature 315 (1985) 207.

[43] S. Solomon, Nature 347 (1990) 347.

[44] O. B. Toon and R. P. Turco, Sci. Am. 264 (1991) 68.

[45] G. P. Brasseur, J. J. Orlando and G. S. Tyndall, Ed., *Atmospheric Chemistry and Global Change*, Oxford University Press (New York, 1999).

[46] M. Akbulut, N. J. Sack and T. E. Madey, Surf. Sci. Report 28 (1997) 177.

[47] W. Weyl, Ann. Phys. (Leipzig) 197 (1863) 601.

[48] J. W. Boag and E. J. Hart, Nature 197 (1963) 45.

[49] A. Migus, Y. Gauduel, J. L. Martin, and A. Antonetti, Phys. Rev. Lett. 58 (1987) 1559.

[50] P. J. Rossky and J. Schnitker, J. Phys. Chem. 92 (1988) 4277.

[51] F. H. Long, H. Lu and K. B. Eisenthal, Phys. Rev. Lett. 64(1990) 1469.

[52] T. Goulet, A. Bernas, C. Ferradini and J.-P. Jay-Gerin, Chem. Phys. Lett. 170 (1990) 492.

[53] E. Neria, A. Nitzan, R. N. Barnett and U. Landman, Phys. Rev. Lett. 67 (1991) 1011.

[54] C. Silva, P. K. Walhout, K.Yokoyama and P. F. Barbara, Phy. Rev. Lett. 80 (1998) 1086.

[55] M. Armbruster, H. Haberland and H.-G. Schindler, Phys. Rev. Lett. 47 (1981) 323.

[56] J. V. Coe, G. H. Lee, J. G. Eaton, S. T. Arnold, H. W. Sarkas, C. Ludewigt, H. Haberland, D. R. Worsnop and K. H. Bowen, J. Chem. Phys. 92 (1990) 3980.

[57] K. W. Oum, M. J. Lakin, D. O. DeHaan, T. Brauers, and B. J. Finlayson-Pitts, Science 279 (1998) 74.

[58] R. Laenen, T. Roth and A. Laubereau, Phys. Rev. Lett. 85 (2000) 50.

[59] P. Kambhampati, D. H. Son, T. K. Kee and P. F. Barbara, J. Phys. Chem. A 106 (2002) 2374.

[60] M. S. Pshenichnikov, A. Baltuska and D. A. Wiersma, Chem. Phys. Lett. 389 (2004) 171.

[61] R. E. Larsen, M. J. Bedard-Hearn and B. J. Schwartz, J. Phys. Chem. B. 110 (2006) 20055.

[62] D. Borgis, P. J. Rossky and L. Turi, J. Chem. Phys. 127 (2007) 174508.

[63] F. Baletto, C. Cavazzoni and S. Scandolo, Phys. Rev. Lett. 95 (2005) 176801.

[64] C. Gahl, U. Bovensiepen, C. Frischkorn and M. Wolf, Phys. Rev. Lett. 89 (2002) 107402.

[65] K. Onda, B. Li, J. Zhao, K. D. Jordan, J. Yang and H. Petek, Science 308 (2005) 1154.

[66] M. Meyer, J. Stähler, D. O. Kusmierek, M. Wolf and U. Bovensiepen, Phys. Chem. Chem. Phys. 10 (2008) 4932.

[67] U. Bovensiepen, C. Gahl, J. Stähler, M. Bockstedte, M. Meyer, F. Baletto, S. Scandolo, X.-Y. Zhu, A. Rubio and M. Wolf, J. Phys. Chem. C 113 (2009) 979.

[68] A. E. Bragg, J. R. R. Verlet, A. Kammrath, O. Cheshnovsky and D. M. Neumark, Science 306 (2004) 669.

[69] D. H. Paik, I. R. Lee, D. S. Yang, J. S. Baskin and A. H. Zewail, Science 306 (2004) 672.

[70] J. R. R. Verlet, A. E. Bragg, A. Kammarath, O. Cheshnovsky and D. M. Neumark, Science 307 (2005) 93.

[71] L. Turi, W. S. Sheu and P. J. Rossky, Science 309 (2005) 914.

[72] T. Sommerfeld and K. D. Jordan, J. Am. Chem. Soc. 128 (2006) 5828.

[73] J. V. Coe, S. T. Arnold, J. G. Eaton, G. H. Lee and K. H. Bowen, J. Chem. Phys. 125 (2006) 014315.

[74] C. W. Luo, Y. T. Wang, F. W. Chen, H. C. Shih anf T. Kobayashi, Opt. Express 17 (2009) 11321.

[75] Q.-B. Lu, Z. Ma and T. E. Madey, Phys. Rev. B58 (1998) 16446.

[76] T. E. Madey, S. A. Joyce, A. L. Johnson and J. A. Yarmoff, in *Desorption Induced by Electronic Transitions DIET IV*, edited by G. Betz and P. Varga, Springer Series in Surface Sciences, Vol. 19 (Springer, Berlin, 1990) 176.

[77] T. L. Gilton, C. P. Dehnbostel and J. P. Cowin, J. Chem. Phys. 91 (1989) 1937.

[78] D. Chakarov and B. Kasemo, Phys. Rev. Lett. 81 (1998) 5181.

[79] Q.-B. Lu and T. E. Madey, Surf. Sci. 451 (2000) 238.

[80] Q.-B. Lu and T. E. Madey, J. Phys. Chem. B105 (2001) 2779.

[81] E. P. Marsh, T. L. Gilton, W. Meier, M. R. Schneider and J. P. Cowin, Phys. Rev. Lett. 61 (1988) 2725.

[82] J. G. Currie and H. Kallio, Lipids 28 (1993) 217.

[83] R. Chaler, R. Vilanova, M. Santiago-Silva, P. Fernandez, J. O. Grimalt, J. Chromatogr. A 823 (1998) 73.

[84] A. Oku, K. Kimura and M. Sato, Chem. Lett. (1988) 1789.

[85] K. Mackenzie, F.-D. Kopinke and M. Remmler, Chemosphere 33 (1996) 1495.

[86] J. Langer, S. Matt, M. Meinke, P. Tegeder, A. Stamatovic and E. Illenberger, J. Chem. Phys. 113 (2000) 11063.

[87] S. Solovev, D. O. Kusmierek and T. E. Madey, J. Chem. Phys. 120 (2004) 968.

[88] Q.-B. Lu and L. Sanche, J. Chem. Phys. 115 (2001) 5711.

[89] Q.-B. Lu and L. Sanche, J. Chem. Phys. 119 (2003) 2658.

[90] Q.-B. Lu and L. Sanche, J. Chem. Phys. 120 (2004) 2434.

[91] R. Marsolais, M., Deschênes and L. Sanche, Rev. Sci. Instrum. 60 (1989) 2724.

[92] I. I. Fabrikant, J. Phys. B 27 (1994) 4325.

[93] I. I. Fabrikant, Phys. Rev. A76 (2007) 012902.

[94] J. M. Von Doren and J. McClellan, J. Chem. Phys. 105 (1996) 104.

[95] A. D. Bass, J. Gamache, L. Parenteau and L. Sanche, J. Phys. Chem. 99 (1995) 6123.

[96] J. C. Polanyi and A. H. Zewail, Acc. Chem. Res. 28 (1995) 119.

[97] A. H. Zewail, Angew. Chem. Int. Ed. 39 (2000) 2587 (Nobel Lecture).

[98] A. D. Bass, J. Gamache, P. Ayotte, and L. Sanche, J. Chem. Phys. 104 (1996) 4258.

[99] N. Nakayama, S. C. Wilson, L. E. Stadelmann, H. L. D. Lee, C. A. Cable and C. R. Arumainayagam, J. Phys. Chem. B 108 (2004) 7950.

[100] A. D. Bass, C. R. Arumainayagam and L. Sanche, Int. J. Mass. Spectrom. 277 (2008) 251.

[101] A. J. Wagner, C. Vecitis and D. H. Fairbrother, J. Phys. Chem. B 106 (2002) 4432.

[102] C. C. Perry, G. M. Wolfe, A. J. Wagner, J. Torres, N. S. Faradzhev, T. E. Madey and D. H. Fairbrother, J. Phys. Chem. B 107 (2003) 12740.

[103] N. S. Faradzhev, C. C. Perry, D. O. Kusmierek, D. H. Fairbrother and T. E. Madey, J. Chem. Phys. 121 (2004) 8547.

[104] CRC Handbrook of Chemistry and Physics, 84th ed, edited by D. R. Lide (CRC Press, Boston, 2003) p.12-131.

[105] H. Tachikawa, Phys. Chem. Chem. Phys. 10 (2008) 2200.

[106] H. Tachikawa and S. Abe, J. Chem. Phys. 126 (2007) 194310.

[107] P. K. Patra and M. Santhanam, Phys. Rev. Lett. 89 (2002) 219803.

[108] R. Müller, Phys. Rev. Lett. 91 (2003) 058502.

[109] R. Müller, J. Chem. Phys. 129 (2008) 027101.

[110] Q.-B. Lu and L. Sanche, Phys. Rev. Lett. 89 (2002) 219804.

[111] C.-R. Wang, K. Drew, T. Luo, M.-J. Lu and Q.-B. Lu, J. Chem. Phys. 129 (2008) 027102.

[112] M. A. Ruderman, H. M. Foley and J. W.Chamberlain, Science 192 (1976) 555.

[113] P. J. Crutzen, Science 189 (1975) 457.

[114] H. Svensmark and E. Friis-Christensen, J. Atmos. Sol.-Terr. Phys. 59 (1997) 1225.

[115] H. Svensmark, Phys. Rev. Lett. 81 (1998) 5027; N. D. Marsh and H. Svensmark, Phys. Rev. Lett. 85 (2000) 5004.

[116] F. Q. Yu and R. P. Turco, J. Geophys. Res. 106 (2001) 4797.

[117] K. S. Carslaw, R. G. Harrison and J. Kirkby, Science 298 (2002) 1732.

[118] R. G. Harrison and D. B. Stephenson, Philos. T. R. Soc. A 462 (2006) 1221.

[119] B. Sun and R. S. Bradley, J. Geophys. Res. 107 (2002) 4211.

[120] J. E. Kristjánsson , C. W. Stjern, F. Stordal, A. M. Fjaeraa, G. Myhre and K. Jonasson, Atmos. Chem. Phys. 8 (2008) 7373.

[121] F. Yu, Atmos. Chem. Phys. 4 (2004) 1037.

[122] E. A. Kasatkina1 and O. I. Shumilov, Annal. Geophys. 23 (2005) 675.

[123] J. R. Pierce and P. J. Adams, Geophys. Res. Lett. 36 (2009) L09820.

[124] H. Svensmark, T. Bondo and J. Svensmark, Geophys. Res. Lett. 36 (2009) L15101.

[125] V. Ramaswamy, M. D. Schwarzkopf and W. J.Randel, Nature 382 (1996) 616.

[126] N. P. Gillett and D. W. Thompson, Science 302 (2003) 273.

[127] V. Ramaswamy, M. D. Schwarzkopf, W. J. Randel, B. D. Santer, B. J. Soden and G. L. Stenchikov, Science 311 (2006) 1138.

[128] N. R. P. Harris, J. C. Farman and D. W. Fahey, Phys. Rev. Lett. 89 (2002) 219801.

[129] J. M. Wareman, R. W. Fessenden and G. Barkale, J. Chem. Phys. 57 (1972) 2702.

[130] M. Allan and T. Skalicky, J. Phys. B 36 (2003) 3397.

[131] J. Kiss, D. Lennon, S. K. Jo and J. M. White, J. Phys. Chem. 95 (1991) 8054.

[132] A. Böttcher and T. Giessel, Surf. Sci. 408 (1998) 212.

[133] J. M. Parnis, L. E. Hoover, D. B. Pedersen and D. D. Paterson, J. Phys. Chem. 99 (1995) 13528.

[134] P. Rawat, V. S. Prabhudesai, M. A. Rahman, N. B. Ram and E. Krishnakumar, Int. J. Mass. Spectrom. 277 (2008) 96.

[135] C. Girardet and C. Toubin, Surf. Sci. Rep. 44 (2001) 163.

[136] Q.-B. Lu, T. E. Madey, L. Parenteau, F. Weik and L. Sanche, Chem. Phys. Lett. 342 (2001) 1.

[137] R. Souda, J. Chem. Phys. 131 (2009) 164501.

[138] V. Ramanathan, L. Callis, R. Cess, J. Hansen, I. Isaksen, W. Kuhn, A. Lacis, F. Luther, J. Mahlamn, R. Reck and M. Schlesinger, Rev. Geophys. 25 (1987) 1441.

[139] IPCC/TEAP 2005 Special Report on Safeguarding the Ozone Layer and the Global Climate System: Issues Related to Hydrofluorocarbons and Perfluorocarbons (Summary for Policy Makers).

[140] D. M. Good, M. Wirtala, G. C. McAlister and J. J., Coon, Mol. Cell. Proteomics 6 (2007) 1942.

Figure Captions

Figure 1. Potential energy curves for dissociative electron attachment (DEA) of a ~0 eV free electron to CF_2Cl_2 in the gas (g) and for dissociative electron transfer (DET) of a weakly-bound pre-solvated electron (e_{pre}^-) to CF_2Cl_2 adsorbed on H_2O ice surface (s). The potential energy curves for the gas phase are constructed from gaseous thermodynamic data, while the curve of $CF_2Cl_2^{*-}$ adsorbed on H_2O ice surface (s) is obtained with the polarization energy of ~1.3 eV (see text).

Figure 2. Schematic diagram for the cosmic-ray driven electron reaction (CRE) mechanism of ozone depletion: cosmic-ray radiation produces an electron in an ice particle in a polar stratospheric cloud (PSC); the electron becomes a precursor (e_{pre}^-) to the solvated electron. e_{pre}^- breaks a halogenated molecule (CFC, HCFC, HCl or $ClONO_2$, etc) to produce a Cl^- ion, which either exists as a free ion or is converted to a Cl_2 molecule by reacting with other species in a PSC in the winter polar stratosphere [12, 14]. Then, the photodetachment of Cl^- or photodissociation of Cl_2 forms one or two Cl atoms that destroy O_3 molecules via (Cl, ClO) reaction cycles when sunlight returns in early spring.

Figure 3. ESDIAD detector with a time of flight (TOF) capability. The gate for the detector is only open just before the desorbing negative ions arrive at the detector [46, 75, 76].

Figure 4. Relative Cl^- yields desorbing from 250 eV primary electrons incident onto various amounts of CF_2Cl_2 covered Ru(0001) at ~25 K as a function of (a) H_2O or (b) NH_3 coverage,

where Cl$^-$ yields are normalized to the initial value at zero H$_2$O/NH$_3$ coverage. Reprinted with permission from [12]. Copyright 1999, the American Institute of Physics.

Figure 5. Relative Cl$^-$ yields desorbing from 250 eV primary electrons incident onto 0.3 ML CF$_2$Cl$_2$ adsorption on top of H$_2$O-precovered Ru(0001) surfaces at ~25 K as a function of the H$_2$O spacer thickness. Reprinted with permission from [12]. Copyright 1999, the American Institute of Physics. The dash-dot line is to extrapolate the Cl$^-$ yield to the H$_2$O spacer thickness of 5 ML, which is at least one order of magnitude less than the maximum Cl$^-$ yield at ~1 ML H$_2$O.

Figure 6. Relative Cl$^-$ yield for various CF$_2$Cl$_2$ precoverages as a function of NH$_3$ coverage. The data in each curve are normalized to the initial value at zero NH$_3$ coverage. (a) Detected by QMS and (b) Detected by ESDIAD. Reprinted with permission from [87]. Copyright 2004, the American Institute of Physics.

Figure 7. Schematic diagram of the electron trapping experiment at ~20 K. A 10 monolayer (ML) Kr film was first deposited onto the Pt substrate; 5 ML H$_2$O was subsequently deposited on the Kr film. Afterward, a submonolayer of electron attaching molecules is adsorbed on top of the H$_2$O film. The variation of the electrostatic potential at the film surface, caused by electron trapping, is monitored by measuring the shift in the energy onset of electron transmission through the film. Reprinted with permission from [90]. Copyright 2004, the American Institute of Physics.

Figure 8. Electron trapping coefficient A$_s$ as a function of electron energy for 0.1 ML CF$_2$Cl$_2$ and 0.1 ML CFCl$_3$: (a) and (b) on 10 ML Kr; (c) and (d) on 5 ML H$_2$O on 10 ML Kr at ~20 K. (a) and (c) reprinted from [13]; (b) and (d) reprinted with permission from [90]. Copyright 2003, the American Institute of Physics.

Figure 9. Electron trapping coefficient A$_s$ as a function of electron energy for 0.1 ML CHF$_2$Cl and 0.1 ML CH$_3$CF$_2$Cl: (a) and (b) on 10 ML Kr; (c) and (d) on 5 ML H$_2$O on 10 ML Kr at ~20

K. (a) and (b) reprinted with permission from [89]. Copyright 2003, the American Institute of Physics; (c) and (d) reprinted with permission from [90]. Copyright 2004, the American Institute of Physics.

Figure 10. (a) Femtosecond transient absorption kinetic traces of the intermediate states XdUs*$^-$ of dissociative electron transfer (DET) reactions of XdUs (X=F, Cl, Br and I) with a pre-solvated electron (e_{pre}^-) at room temperature, pumped at 320 nm and probed at 330 nm: e_{pre}^- + XdU$\rightarrow$ XdU*$^-$ $\rightarrow$X$^-$ + dU$^\bullet$. The sharp peak at time zero for the pure water trace (solid line) is the coherent spike. For XdUs, the symbols are the experimental data, while the solid lines are the best fits to the measured data. Reproduced with permission from [21]. Copyright 2007, Wiley-VCH Verlag GmbH & Co. KGaA. (b) Schematic diagram for the DET reaction of two e_{pre}^- states with IdU. Reproduced with permission from [28]. Copyright 2008, the Royal Society of Chemistry.

Figure 11. (a) Lifetime of the presolvated electron state as a function of the coverage of CFCl$_3$ adsorbed on 5 ML H$_2$O/Ag(111). (b) Schematic diagram for the fate of the photoinjected electron in CFCl$_3$/H$_2$O/Ag(111): photoinjection of electron into the loosely bound e_{pre} state residing below the vacuum level (***a***); solvation in the ice layer (***b***); back transfer of the photoinjected electron to the metal (***c***); electron transfer to coadsorbed CFCl$_3$ (***d***). Reprinted with permission from [16]. Copyright 2006, the American Chemical Society.

Figure 12. 2PPE spectroscopy performed on crystalline D$_2$O (coverage ∽4.5 BL) deposited on Ru(001) at ∽30 K. (a) represents a 2D plot of the 2PPE intensity in false color as a function of both $E - E_F$ and the coverage of CFCl$_3$. (b) shows vertical cuts of the 2D plot (2PPE intensity

versus $E - E_F$) for different CFCl$_3$ coverages. The dashed spectrum is a 2PPE spectrum realized on 4.5 BL of freshly deposited crystalline D$_2$O before CFCl$_3$ adsorption. Reprinted with permission from [17]. Copyright 2009, the Royal Society of Chemistry.

Figure 13. (a) Cosmic-ray (CR) intensity and monthly mean total ozone in pre-ozone hole (Oct. 1979 for Antarctica and March 1979 for Arctic) and ozone hole period (dashed line for Oct. 1998 for Antarctica and March 1998 for Arctic) versus latitude. (b) Cosmic-ray ionization rate and ozone loss versus altitude: the curve for the spring ozone hole over Syowa, Antarctica, was obtained by subtracting the altitude distribution curve of pre-ozone hole from that of ozone-hole period [14].

Figure 14. (a) Percentage variations of observed CR intensity and annual average zonal-mean total ozone with latitudes 0-60°S; (b) Percentage variations of observed CR intensity and monthly average zonal mean total ozone in October Antarctic with latitudes of 60-90° S during the period of 1990-2008. The O$_3$ data are relative to the value at 1992. Updated from Lu [15], where the zonal mean total O$_3$ data for October 2008 (upper triangle, green) was predicted.

Figure 15. (a) Percents of 3-month (October-December) average zonal mean total O$_3$ over Antarctica with latitudes of 60-90° S, normalized to [O$_3$]$_0$=375 DU, and the equivalent effective stratospheric chlorine (EESC) over Antarctica during the period of 1979-2008. Observed O$_3$ data (solid circles) were obtained from NASA N7/M3/EP/OMI satellite datasets; the solid line through the data points is a 3-point average smoothed curve to aid the eyes. The EESC data were obtained from WMO Report [37]. (b) October Antarctic (60°S to 90°S) total column ozone

anomalies from various two-dimensional (2-D) and three-dimensional (3-D) coupled (photo)chemistry-Climate Models (CCMs) (colored lines) [from Fig. 6-12 in ref. 37]. Note that in (b) the vertical dash line in red corresponds to the year 2008, where several CCMs predicted a minimum Antarctic ozone hole, which is exactly opposite to the observed data in (a).

Figure 16. (a) Percent of spring zonal-mean total ozone over Antarctica with latitudes of 60-90° S and cosmic ray (CR) intensity variation during the period of 1979-2008, as well as total ozone variation given by the CRE model (Eq. 7 with $k=2.1 \times 10^{-9}$). The spring total ozone data are the same as those in Fig. 15(a), while the CR data were obtained from the measurements at McMurdo (77.9^{o} S, 166.6^{o} E). The upper triangle is the ozone data predicted by Eq. (7) for 2009. (b) Similar to (a), but the ozone data were obtained from the Antarctic Halley (75°35'S, 26°36'W) and averaged from September to November, normalized to $[O_3]_0 = 300$ DU; the calculated ozone data were obtained by Eq. (7) with $k=2.8 \times 10^{-9}$. (c) The summer zonal-mean total ozone (solid circles) at 60-90° S averaged from January and February and the summer ozone data (solid triangles) at Halley averaged from January to March, normalized to $[O_3]_0 = 320$ DU. In (a)-(c), the fine solid lines through the data points are 3-point average smoothed curves to aid the eyes.

Figure 17. Temperatures at the lower Antarctic stratosphere (100 hPa) and total ozone observed at Halley (75°35' S, 26°36' W) from 1956 to 2008: (a) during the winter (June-August, prior to the Antarctic ozone hole season), (b) the later spring (November, after the ozone hole peak) and (c) annual mean. In (a), the data for the cosmic ray (CR) intensities at McMurdo (77.9^{o} S, 166.6^{o} E) from 1969 to 2009 are also shown, while in (b) and (c), the total O_3 data fitted by Eq. (7) with

the EESC values from WMO Report [37] are also shown. Note that no O_3 data are shown in (a), as they are not available in the winter Antarctic stations. A 3-point average smoothing was applied to the observed ozone data in (b) and (c) and the temperature data in (a)-(c).

Figure 18. Temperatures at the lower Antarctic stratosphere (100 hPa) as a function of total ozone observed at Halley (75°35' S, 26°36' W): (a) November data spanning from 1956 to 2008 (Fig. 17b) and (b) Annual data from 1979 to 2008 (Fig. 17 c). The solid lines are the linear fits to the observed data, giving the correlation coefficients R=0.94 (a) and R=0.89 (b) and the probability (that R is zero) P<0.0001.

Figure 19. (April, June, August, September) monthly mean CH_4 level in ppmv combined CLEAS and HALOE datasets on UARS, which are representative of the entire UARS record (repeating seasonal cycles were fit through an over six year record from 1992 to 1998), and April and August 1992 monthly mean CF_2Cl_2 level in pptv from CLEAS (only the 1992 data available).

Figure 20. Future trends of (a) cosmic ray (CR) intensity, (b) the equivalent effective stratospheric chlorine (EESC) and (c) total ozone over Antarctica with latitudes (60-90° S). The future CR data in (a) were obtained by Eq. (8) through the best fit to all the observed data at McMurdo from 1969 to 2009, while the EESC data in (b) were obtained from WMO Report [37]. In (c), the observed total ozone (solid circles) from 1979 to 2008 are the same as those in Fig. 15(a) and 16(a), while the calculated total ozone data (solid line) were obtained by Eq. (7) with the CR curve in (a) and EESC curve in (b).

Figure 21. Variations of observed southern hemisphere (SH), northern hemisphere (NH) and global surface temperatures and the normalized equivalent effective stratospheric chlorine (EESC) from 1850 to 2008. The solid curves in black and red are the original observed data and their 3-point average smoothing of surface temperatures, respectively. The EESC for SH, NH and global stratospheres are respectively obtained with the assumed time delays Γ=8, 9 and 9 years from the surface halogen peak at 1994.

Figure 22. (a) Global temperature variation (ΔT) versus normalized equivalent effective stratospheric chlorine (EESC) with the data over 1970-2008, where $\Delta T=T-T_{80}$ (T_{80} is the temperature in 1980) and the EESC values are normalized to its value in 1980; the solid line is the linear fit to the observed data, giving $\Delta T=-0.31+0.30\times EESC$ (^{o}C) with the correlation coefficient R=0.89 and the probability (that R is zero) P<0.0001. (b) Time-series vvariations of global surface temperature and cosmic-ray (CR) intensity over 1970-2008 and EESC from 1970 to 2050, relative to 1980; a 3-point average smoothing was applied to observed surface temperature data. A global cooling is projected for the coming five decades.
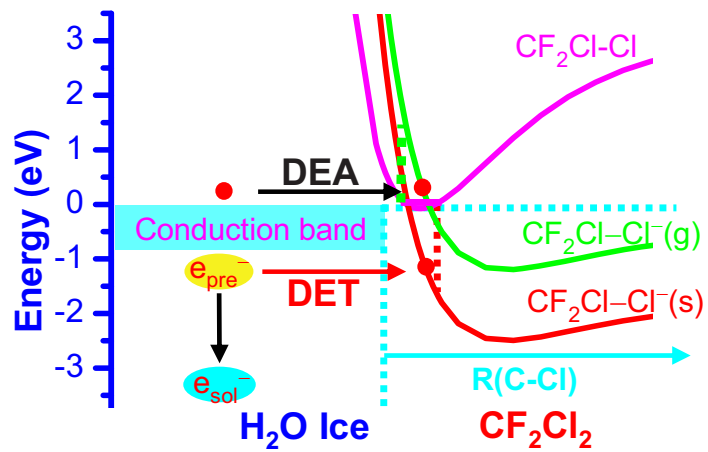
Lu, Physics Reports, Figure 1
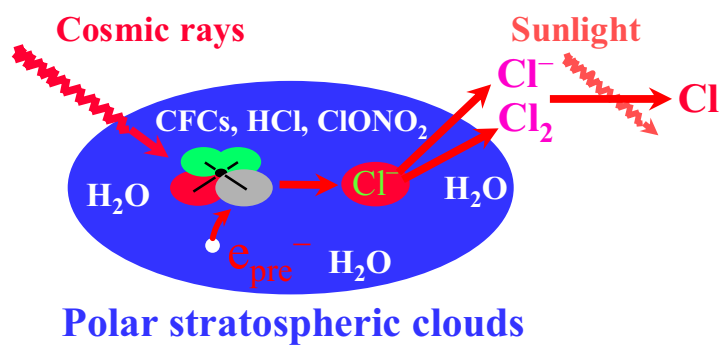
Lu, Physics Reports, Figure 2
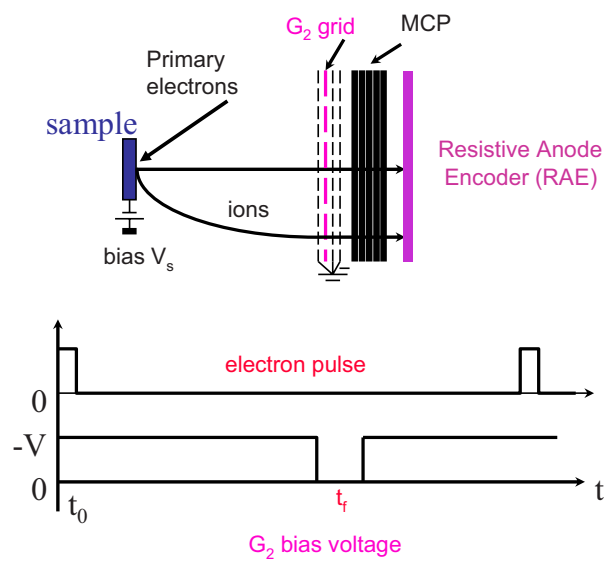
Lu, Physics Reports, Figure 3
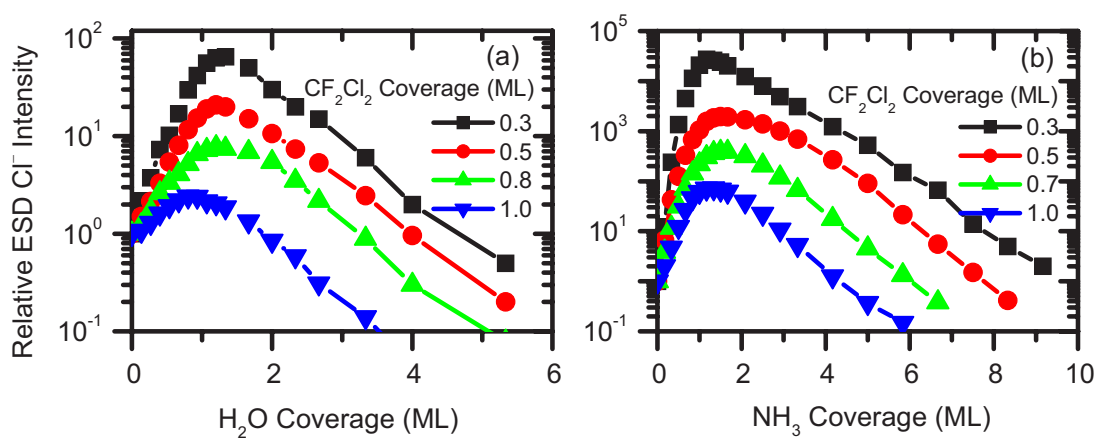
Lu, Physics Reports, Figure 4
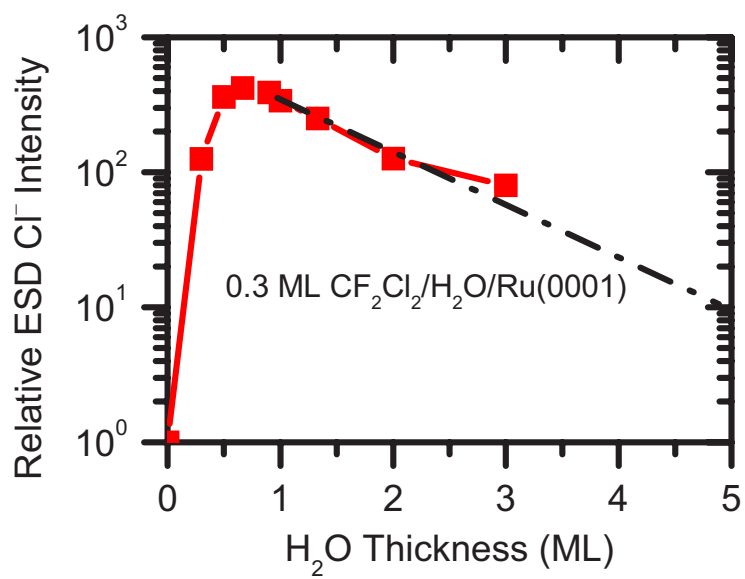
Lu, Physics Reports, Figure 5
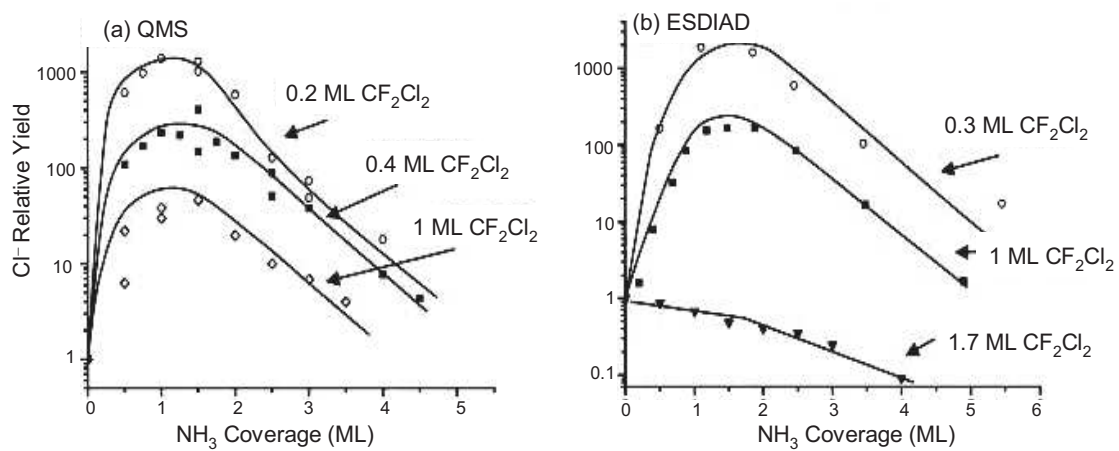
Lu, Physics Reports, Figure 6
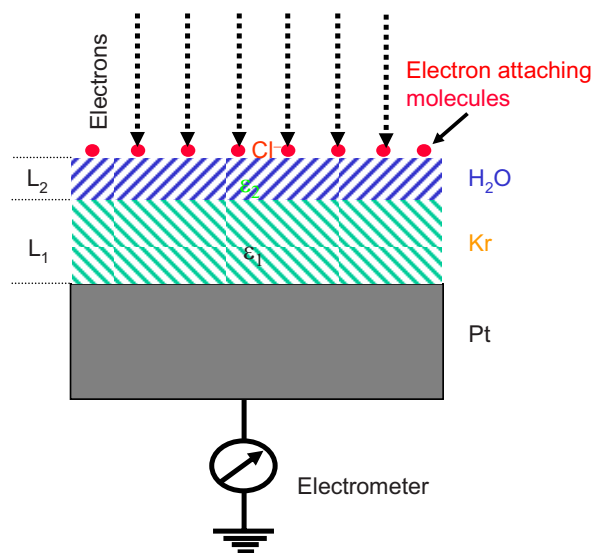
Lu, Physics Reports, Figure 7
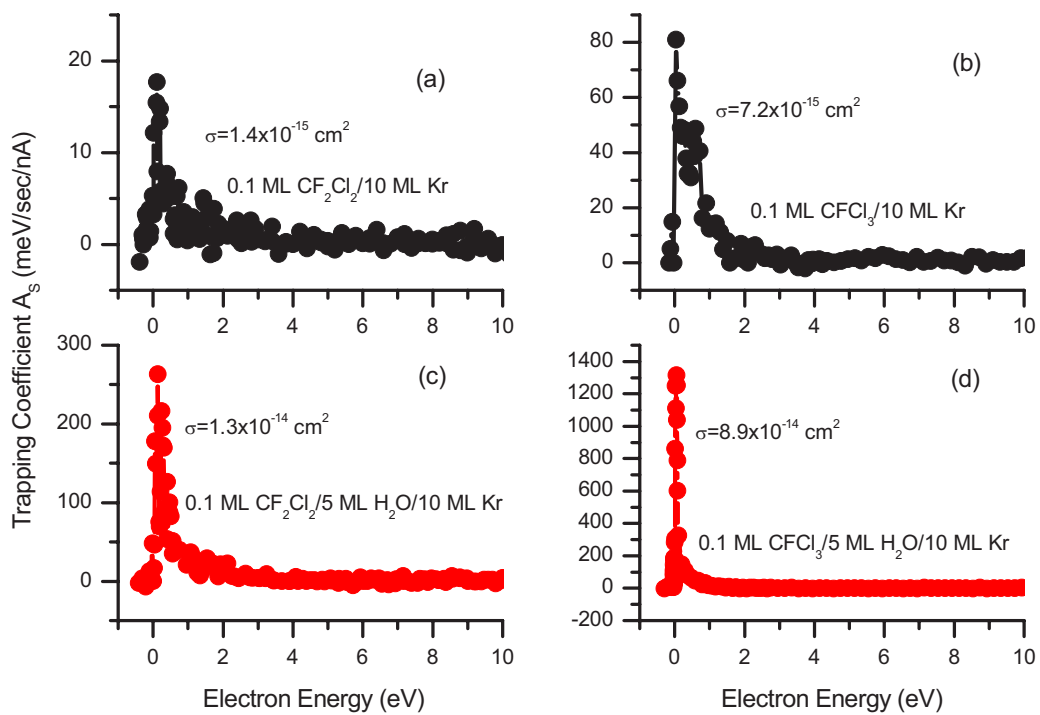
Lu, Physics Reports, Figure 8
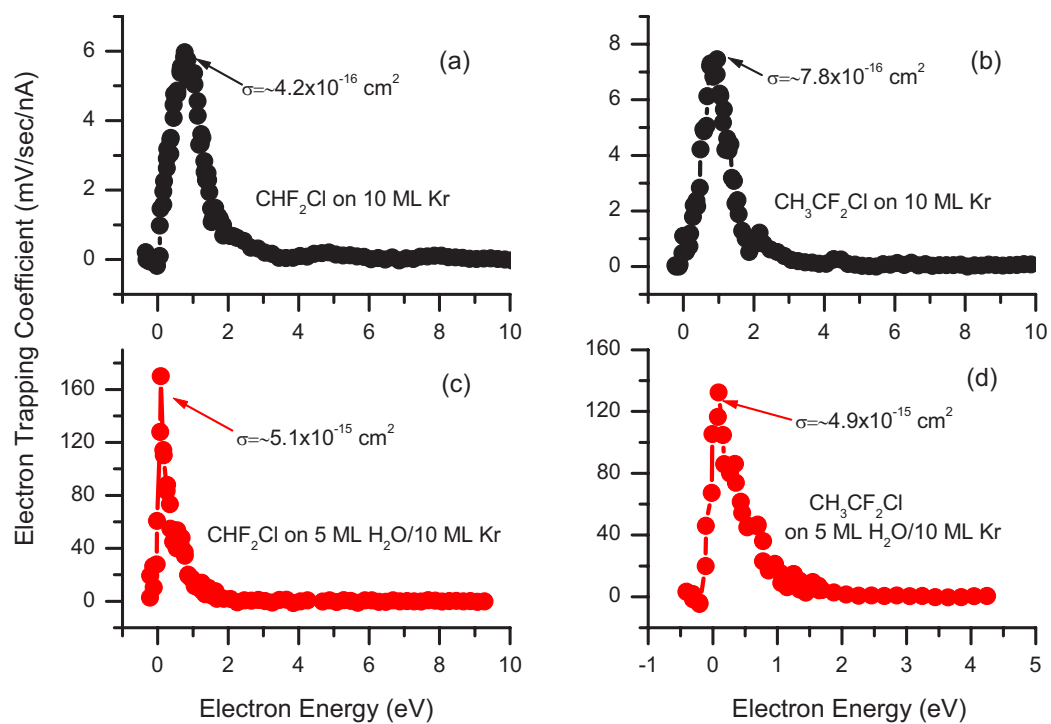
Lu, Physics Reports, Figure 9
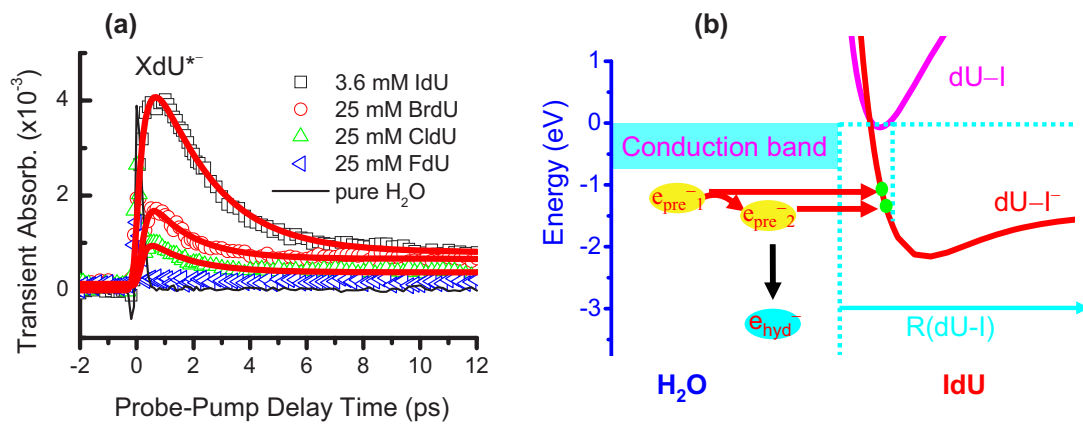
Lu, Physics Reports, Figure 10
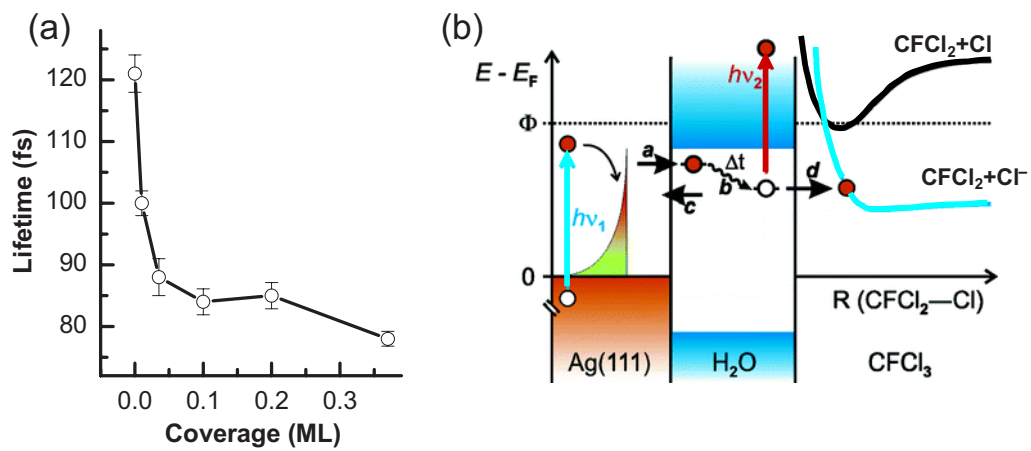
Lu, Physics Reports, Figure 11
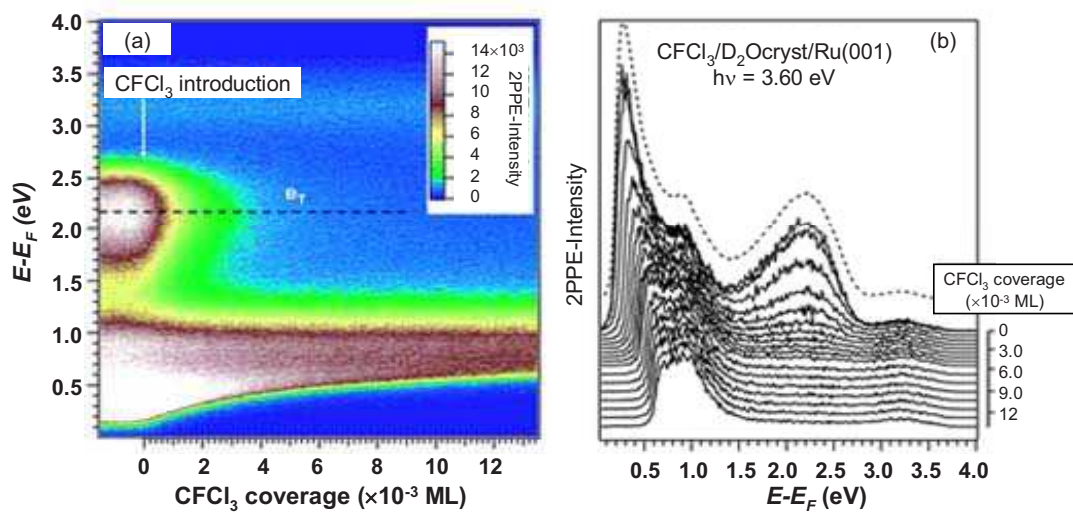
Lu, Physics Reports, Figure 12
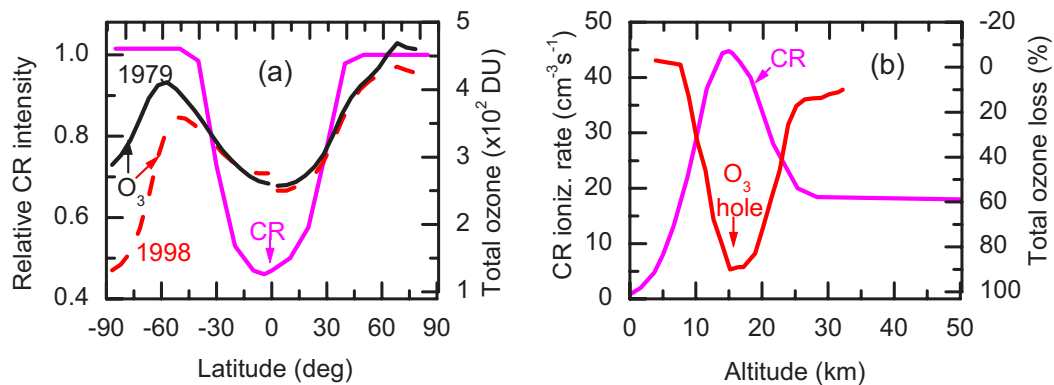
Lu, Physics Reports, Figure 13
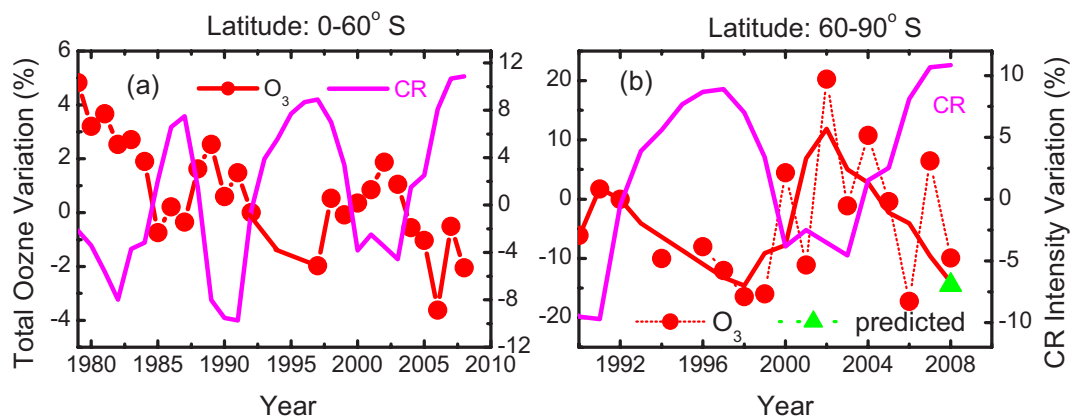
Lu, Physics Reports, Figure 14
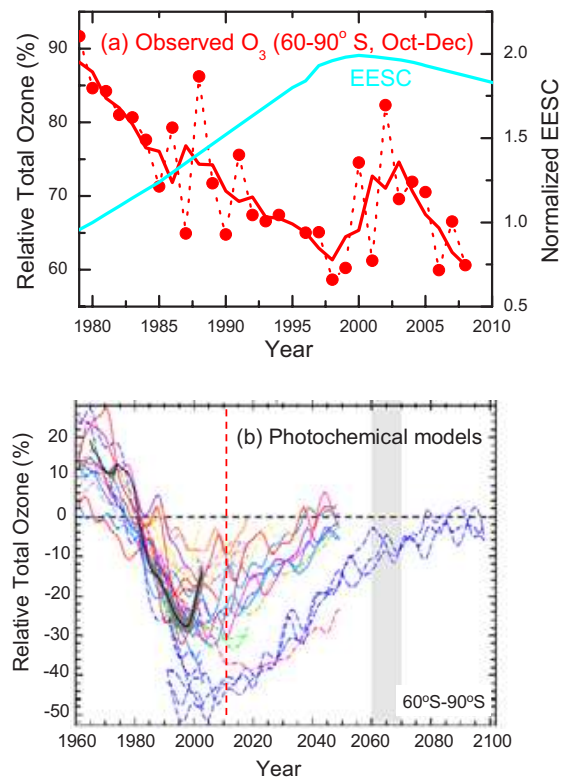
Lu, Physics Reports, Figure 15
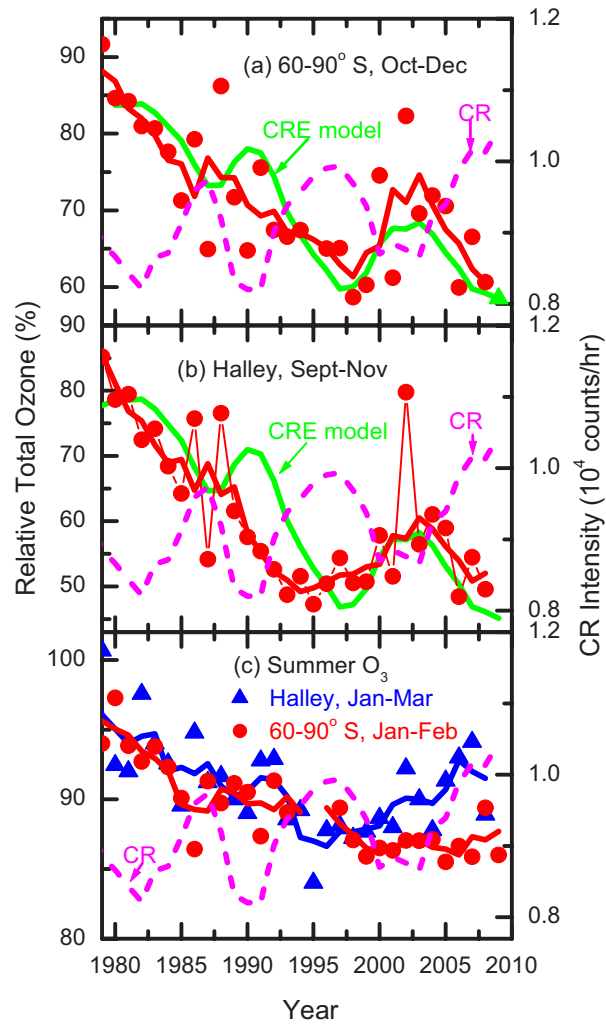
Lu, Physics Reports, Figure 16
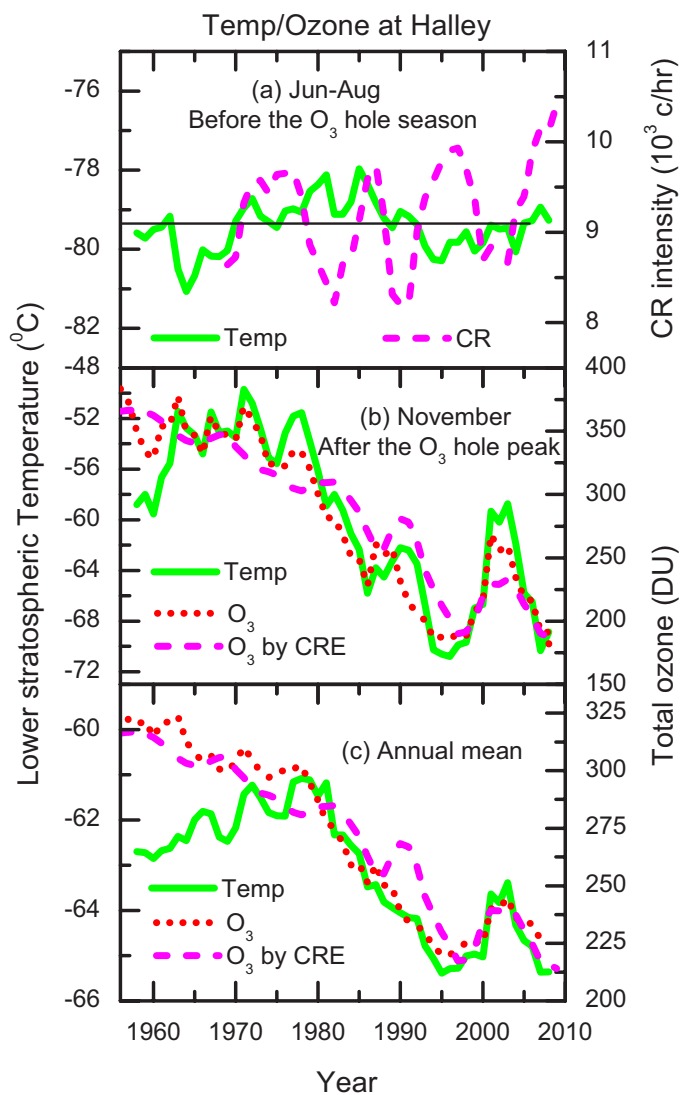
Lu, Physics Reports, Figure 17
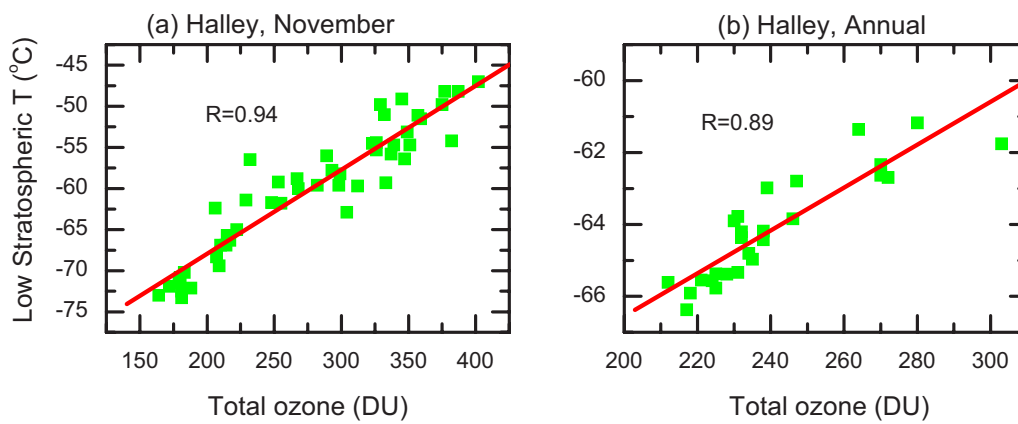
Lu, Physics Reports, Figure 18
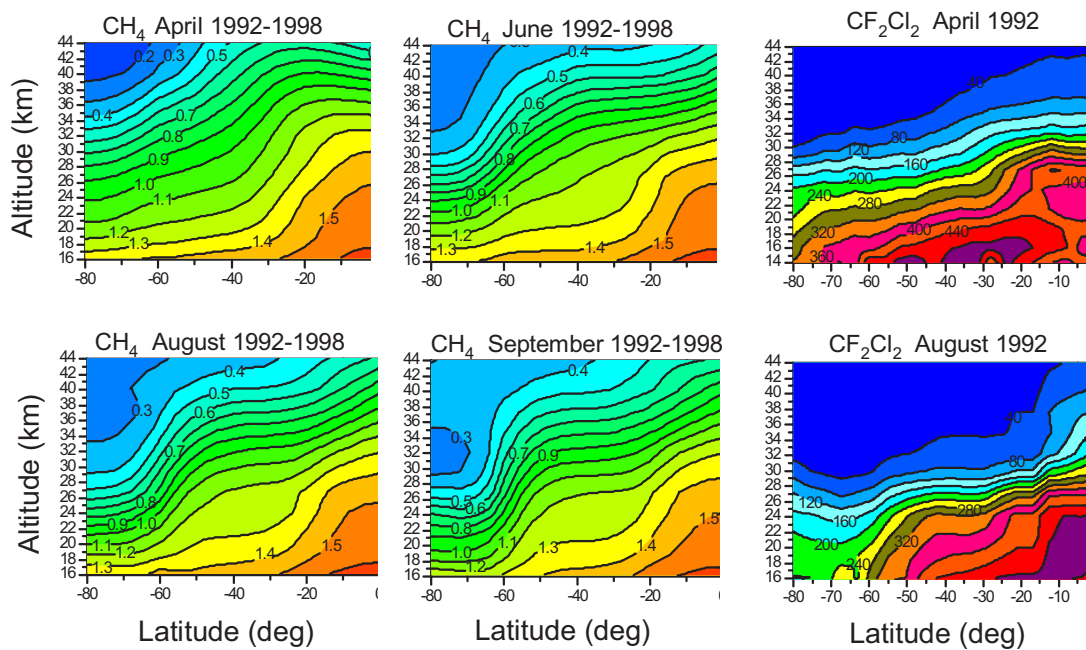
Lu, Physics Reports, Figure 19
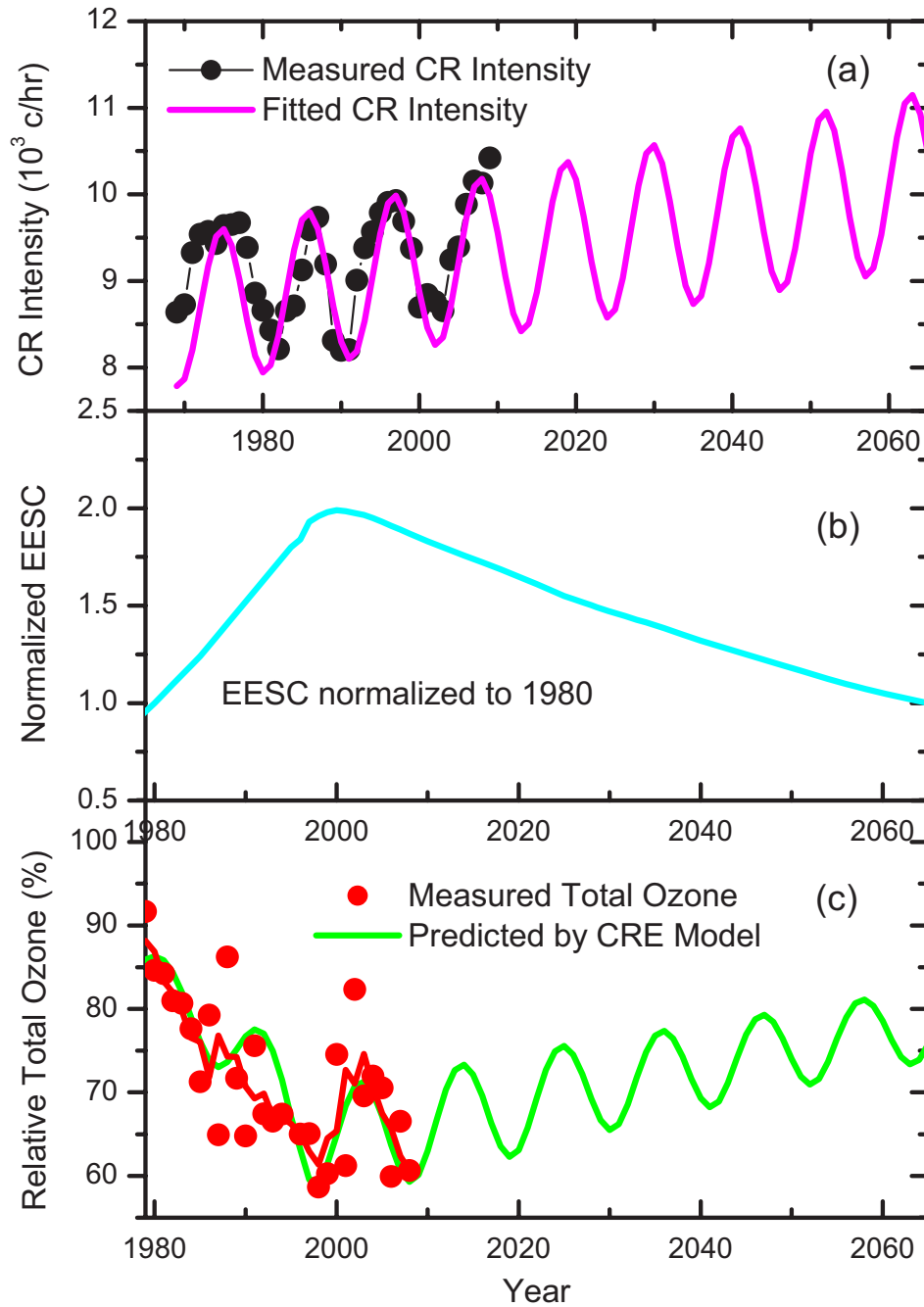
Lu, Physics Reports, Figure 20
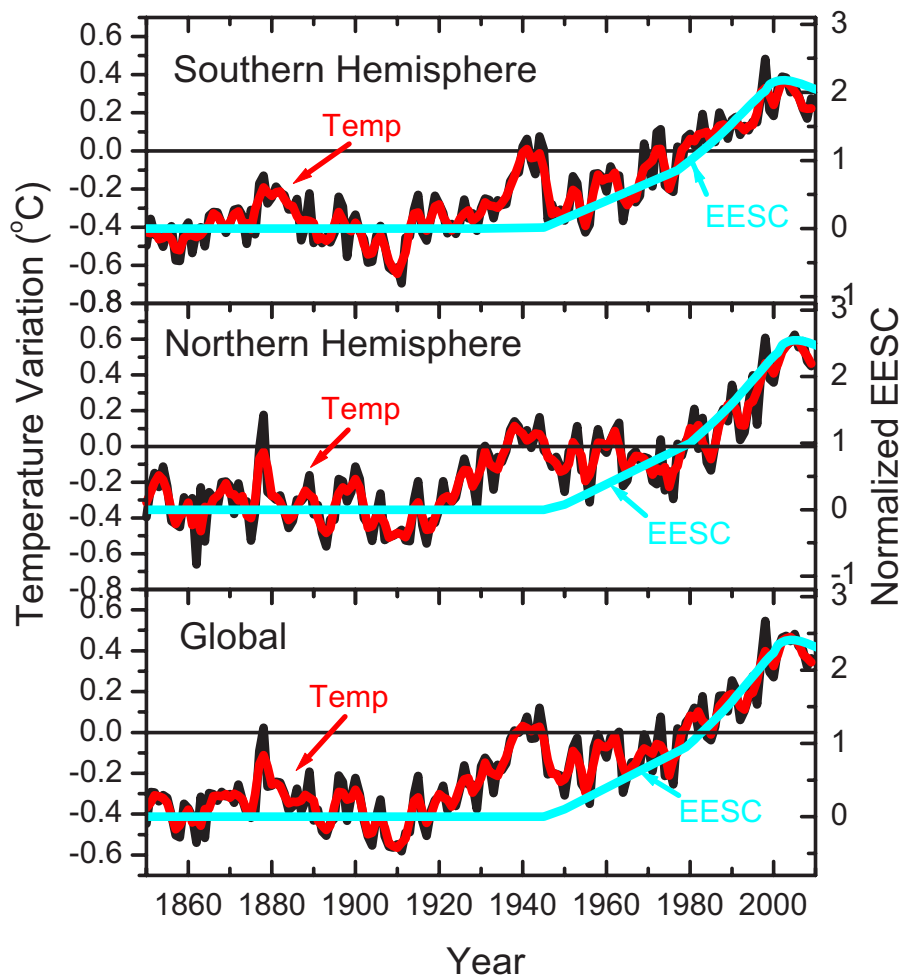
Lu, Physics Reports, Figure 21

Lu, Physics Reports, Figure 22